



ELSEVIER

Discrete Mathematics 192 (1998) 41–80

**DISCRETE
MATHEMATICS**

Fullerenes and coordination polyhedra versus half-cube embeddings¹

Antoine Deza^{a,b,*}, Michel Deza^c, Viatcheslav Grishukhin^d^a *Ecole Polytechnique Fédérale de Lausanne, département de mathématiques, CH-1015 Lausanne, Suisse*^b *Ecole des Hautes Etudes en Sciences Sociales, Centre d'analyse et de Mathématiques sociales, 54 Bld Raspail, Paris, France*^c *CNRS, Ecole Normale Supérieure, département de mathématiques et informatique, 45 rue d'Ulm, Paris, France*^d *CEMI, Russian Academy of Sciences, Krasikova 32, Moscow 117 418, Russia*

Received 17 September 1996; revised 29 March 1997; accepted 10 October 1997

Abstract

A fullerene F_n is a 3-regular (or cubic) polyhedral carbon molecule for which the n vertices — the carbon atoms — are arranged in 12 pentagons and $(n/2 - 10)$ hexagons. Only a finite number of fullerenes are expected to be, up to scale, isometrically embeddable into a hypercube. Looking for the list of such fullerenes, we first check the embeddability of all fullerenes F_n for $n < 60$ and of all preferable fullerenes C_n for $n < 86$ and their duals. Then, we consider some infinite families, including fullerenes with icosahedral symmetry, which describe virus capsids, onion-like metallic clusters and geodesic domes. Quasi-embeddings and fullerene analogues are considered. We also present some results on chemically relevant polyhedra such as coordination polyhedra and cluster polyhedra. Finally we conjecture that the list of known embeddable fullerenes is complete and present its relevance to the Katsura model for vesicles cells. © 1998 Published by Elsevier Science B.V. All rights reserved

1. Introduction and basic properties

1.1. Introduction

A *fullerene* is a carbon molecule which can be seen as a *simple* polyhedron (i.e. each vertex has exactly 3 neighbouring vertices), we denote it by F_n in honour of the pioneer, R.B. Fuller, and the expert, P.W. Fowler. The n vertices — the carbon atoms — are arranged in 12 pentagons and $(n/2 - 10)$ hexagons and the $\frac{3}{2}n$ edges correspond to carbon-carbon bonds. Fullerenes F_n can be constructed for all even $n \geq 20$ except $n = 22$ [37, pp. 271, 51]. For a given n , different arrangements of

* Corresponding author. E-mail: deza@masgl.epfl.ch.

¹ Research supported for the first author by EC program Human Capital and Mobility, DIMANET contract ERBCHRXCT 94-0429.

facets are possible; for example, there are 1, 1, 1, 2, 3, 40, 271 and 1812 fullerenes F_n for $n = 20, 24, 26, 28, 30, 40, 50$ and 60, respectively (see, for example, [5] where a detailed list of number of isomers is given). Among isomers, fullerenes without pair of pentagons sharing a common edge are denoted by C_n and called *preferable* (or also IP, for Isolated Pentagon fullerenes). For example, the unique preferable fullerene made of 60 carbon atoms C_{60} is the truncated icosahedron (a semi-regular or Archimedean solid) also called *buckminsterfullerene*. A usual way to somehow distinguish between isomers is to give their symmetry group. For example, $C_{180}(I_h)$ is the unique preferable fullerene with 180 vertices and symmetry group I_h (extended icosahedral group of order 120). While $C_{60}(I_h)$ is a soccer ball, $C_{70}(D_{5h})$ and $C_{84}(D_{2d})$ respectively resemble a rugby and a baseball ball. The general references are Fowler and Manolopoulos [28] for fullerenes and Grünbaum [37] for polyhedra. References for so-called *point groups* is [59], and [29,37] for operations on polyhedra such as pentakis, leapfrog, truncation and dual. In this paper we focus on the following metric question.

Can we embed into a hypercube the graph formed by the vertices and the edges of a fullerene (and other chemically relevant polyhedra) while preserving, up to a scale, the path distances?

Before recalling some graph related metric notions, we briefly discuss the relevance of such embeddings. To determine if a fullerene F_n can be isometrically embedded into a hypercube H_m or into a half-cube $\frac{1}{2}H_m$, for example for the half-cube embedding, means that we can label or encode the vertices of F_n by a binary string of length m with an even number of ones such that the square of the Euclidean distance between those addresses is twice the path distance of the vertices in the skeleton of the original fullerene. We recall that the half-cube $\frac{1}{2}H_m$ is the graph defined on the vertices of the hypercube H_m with an even number of coordinates equal to 1, two vertices x, y being adjacent if their Hamming distance is 2, i.e. if: $|\{i \in \{1, \dots, m\}: x_i \neq y_i\}| = 2$. If moreover, the embedding is ℓ_1 -rigid, as for $F_{20}(I_h)$ and $C_{80}(I_h)$, then we have an essentially unique encoding (see the end of Section 1.1 and [15] for details). Such labelling of vertices can also be useful for the nomenclature of fullerenes [24] and for the calculation of molecular parameters depending only on the graphical distances such as the Wiener, J , and other indices [3].

The *path metric* d_G associated with a connected graph $G(V, E)$ is the integer valued metric on the vertices of G defined by setting $d_G(v_1, v_2)$ equal to the length of the shortest path in G joining v_1 to v_2 . An ℓ_1 -graph is a graph G for which the path metric d_G is, up to a scale λ , isometrically embeddable into a hypercube H_m . That is, for some $\lambda, m \in \mathbb{N}$, there is a mapping $\phi : V \rightarrow H_m$ such that

$$\lambda d_G(v_i, v_j) = \|\phi(v_i) - \phi(v_j)\|_{\ell_1} = \sum_{k=1}^m |\phi_k(v_i) - \phi_k(v_j)|$$

with $v_i \in V$ and $\phi(v_i) = \{\phi_1(v_i), \dots, \phi_m(v_i)\} \in H_m$. Such smallest integer λ is called the *scale* of the embedding. We say that a polyhedron P is ℓ_1 -embeddable if its skeleton $G(P)$, i.e. the graph formed by its vertices and edges, is an ℓ_1 -graph.

Clearly, the embeddability into an n -cube implies the embeddability into the half-cube $\frac{1}{2}H_{2n}$. Moreover, with a *isometric subgraph* being a subgraph preserving the distances, for any graph G ℓ_1 -embeddable up to scale λ into a hypercube, we have:

- (i) $\lambda = 1 \Leftrightarrow G$ is an isometric subgraph of a hypercube, we write: $G \rightarrow H_m$
- (ii) $\lambda = 1$ or $2 \Leftrightarrow G$ is an isometric subgraph of a half-cube, we write: $G \rightarrow \frac{1}{2}H_m$.

Lemma 1.1 (Chepoi et al. [9]). *The scale λ of a planar ℓ_1 -graph is either 1 or 2.*

All ℓ_1 -metrics on n vertices (i.e all ℓ_1 -metric spaces (d, V_n) with $|V_n| = n$) form a $\binom{n}{2}$ -dimensional pointed cone called the *cut cone*. This cone is generated by the $2^{n-1} - 1$ nonzero *cut metrics* $\delta(S)$ defined for a given subset S of $V_n = \{1, 2, \dots, n\}$ by $\delta(S)_{ij} = 1$ if exactly one of i, j is in S and 0 otherwise, for $1 \leq i < j \leq n$ (cut metrics are also sometimes called *split metrics*, see [20]). In other words, a graph G (or any metric) is ℓ_1 -embeddable if the path metric d_G is a nonnegative linear combination of cuts:

$$d_G = \sum_{S \subset V_n} a_S \delta(S) \quad \text{with} \quad a_S \geq 0 \text{ for all } S.$$

If the embedding is essentially unique, i.e. if the above linear combination is unique up to an isomorphism, the graph is called *ℓ_1 -rigid* [14]. Restated in terms of cone, a metric is ℓ_1 -rigid if and only if it belongs to a simplex face of the cut cone. For example, see Lemma 2.1, the embeddings of F_{20} into $\frac{1}{2}H_{10}$ and of its dual F_{20}^* into $\frac{1}{2}H_6$ are ℓ_1 -rigid.

Lemma 1.2 (Chepoi et al. [9]). *Any ℓ_1 -graph not containing K_4 is ℓ_1 -rigid.*

Finally, we recall that a graph G is called *hypermetric* (see [15] for details) if its path metric d_G satisfies all *hypermetric inequalities* defined by

$$\sum_{1 \leq i < j \leq n} b_i b_j d_G(i, j) \leq 0 \tag{1}$$

where $b = \{b_1, b_2, \dots, b_n\} \in Z^n$ and $\sum_{i=1}^n b_i = 1$. With $\sum_{i=1}^n |b_i| = 2k + 1$, this inequality is called a $(2k + 1)$ -gonal inequality and a graph satisfying all $(2k + 1)$ -gonal inequalities is called $(2k + 1)$ -gonal. For a path metric of a graph G , the links between those metric properties are given by the following inclusions [15]:

$$\begin{aligned} G \text{ is an isometric subgraph of a hypercube} &\Rightarrow d_G \text{ is } \ell_1\text{-rigid} \\ &\Rightarrow G \text{ is an isometric subgraph of a half-cube} \Rightarrow d_G \text{ is an } \ell_1\text{-graph} \\ &\Rightarrow d_G \text{ is hypermetric} \Rightarrow d_G \text{ is } (2k + 1)\text{-gonal} \Rightarrow d_G \text{ is } (2k - 1)\text{-gonal} \\ &\Rightarrow d_G \text{ is 3-gonal (= metric)}. \end{aligned}$$

We also recall that Djoković [19] gave a characterization of ℓ_1 -graphs with scale $\lambda = 1$ which can be reformulated [1] in the following way: a graph is an isometric

Table 1
Isoperimetric quotient of Platonic solids

m	Polyhedron P	$IQ(P)$	Upper bound \overline{IQ}_m
4	Tetrahedron	$\frac{\pi}{6\sqrt{3}} \simeq 0.302$	$\frac{\pi}{6\sqrt{3}}$
6	Cube	$\frac{\pi}{6} \simeq 0.524$	$\frac{\pi}{6}$
8	Octahedron	$\frac{\pi}{3\sqrt{3}} \simeq 0.605$	$\simeq 0.637$
12	Dodecahedron	$\frac{\pi\tau^{7/2}}{3.5^{5/4}} \simeq 0.755$	$\frac{\pi\tau^{7/2}}{3.5^{5/4}}$
20	Icosahedron	$\frac{\pi\tau^4}{15\sqrt{3}} \simeq 0.829$	$\simeq 0.851$

subgraph of a hypercube if and only if it is bipartite and 5-gonal. A graph G is an ℓ_1 -graph if and only if G is an isometric subgraph of a Cartesian product of cocktail-party graphs (i.e. dual hypercube graph) and half-cube graphs, see [62] (or [12] for another proof). As for complexity results: while recognizing a metric as ℓ_1 -embeddable (i.e., isometrically embeddable into an ℓ_1^m) implies it is NP-complete [42,2], recognizing a graph as ℓ_1 -embeddable implies it is polynomial [16]. See also [15] for a general study of ℓ_1 -metrics.

1.2. Fullerenes and the isoperimetric problem for polyhedra

1.2.1. The isoperimetric quotient

Fullerenes are closely related to the isoperimetric problem for polyhedra (which goes back to works of Lhuillier in 1782, see [48]). This problem is to find the polyhedron with a given surface S and m facets which contains the largest volume V . In other words, minimize the Steinitz number S^3/V^2 or, equivalently, maximize the *isoperimetric quotient* $IQ = 36\pi V^2/S^3$ — a term introduced by Pólya in [56, Chap. 10, Problem 43]. See Florian [26] for a survey and recall the classical isoperimetric inequality for solids: $36\pi V^2/S^3 \leq 1$, with equality only for the sphere. The polyhedron P_m with m facets with largest IQ is called *best* polyhedron with m facets. For example, the regular tetrahedron, cube and dodecahedron are the best polyhedra with, respectively, 4, 6 and 12 facets. The IQ of the five Platonic solids increases as given in Table 1 where $\tau = (1 + \sqrt{5})/2$ denotes the golden ratio and the upper bound \overline{IQ}_m of Fejes Tóth–Goldberg is the one given in Theorem 37 of [26]. This bound is sharper than the one given in [34]: $IQ(P_m) \leq (m - 2)^2/m(m - 1)$.

Kepler [44] interpreted a high (resp. low) IQ as wetness (resp. dryness) and as a justification for why the icosahedron and the tetrahedron symbolizes respectively the water and the fire, see Fig. 1.

1.2.2. Fullerenes and their duals: best polyhedral approximation of a sphere?

In [34] Goldberg introduced, in 1935, in a slightly more general setting, the fullerenes (he mentions that Kirkman [46] found, in 1882, over 80 out of the 89 isomers of F_{44}). He defined, for $n \neq 18, 22$, a *medial polyhedron* with n vertices as a simple polyhedron

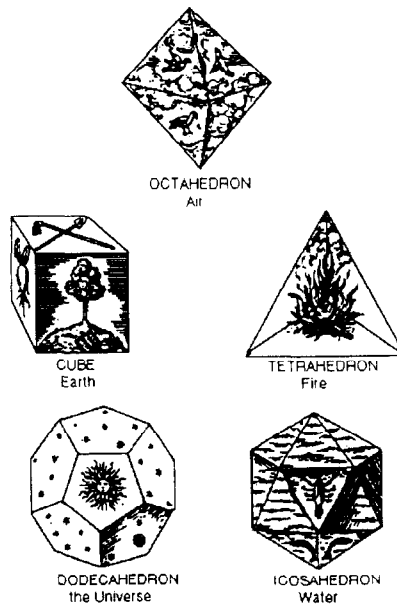


Fig. 1. The five Platonic solids (adapted from a drawing by Kepler).

for which all facets are $\lfloor 6 - \frac{24}{n+4} \rfloor$ -gons or $\lfloor 7 - \frac{24}{n+4} \rfloor$ -gons. Clearly, for $4 \leq n \neq 18 \leq 20$, the first 8 medial polyhedra are the 8 dual convex deltahedra and, for $20 \leq n \neq 22$, medial polyhedra are the fullerenes. Therefore, we extend the notation F_n to a medial polyhedron with n vertices. Fig. 2 reproduces those medial polyhedra, the last 9 being $F_{20}(I_h)$, $F_{24}(D_{6d})$, $F_{26}(D_{3h})$, $F_{28}(T_d)$, $F_{28}(D_2)$, $F_{36}(D_{3h})$, $F_{36}(D_{6h})$, $C_{60}(I_h)$ and $C_{80}(I_h)$ (called in [34] *chamfered dodecahedron*). For example, $IQ(P) \simeq 0.755, 0.906$ and 0.928 for $P = F_{20}(I_h)$, $C_{60}(I_h)$ and $C_{80}(I_h)$.

Goldberg [34] proved that the regular dodecahedron $F_{20}(I_h)$ is the best polyhedron with 12 facets and gave the following conjecture.

Conjecture 1.3 (Goldberg [34]). Among polyhedra with m facets, $m \neq 11, 13$, a medial polyhedron $F_{2(m-2)}$ reaches the highest IQ.

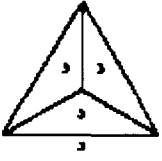
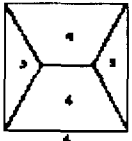
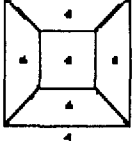
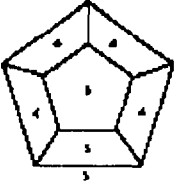
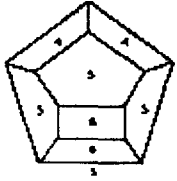
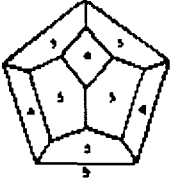
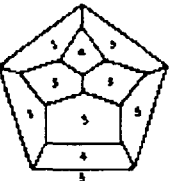
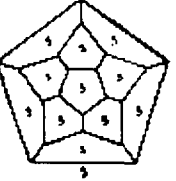
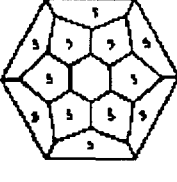
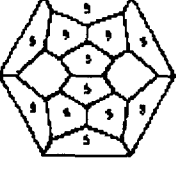
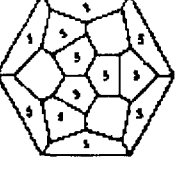
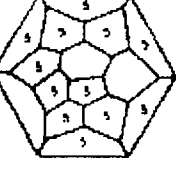
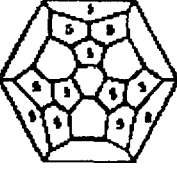
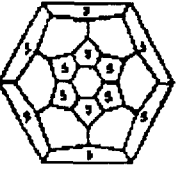
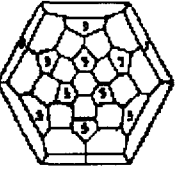
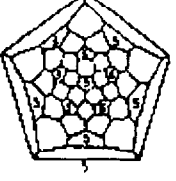
We also recall the Grace [36] and Steiner [63] conjectures.

Conjecture 1.4 (Grace [36]). Among all polyhedra with n vertices lying on the unit sphere, $n \neq 18, 22$, a dual medial polyhedron F_n^* reaches the highest volume.

Conjecture 1.5 (Steiner [63]). Each of the five Platonic solids reaches the highest IQ among combinatorially equivalent polyhedra.

The Steiner conjecture is still open for the icosahedron. If we allow any combinatorial type, medial polyhedra F_{12} and $F_{36}(D_{6h})$ (i.e. VIII and XX–2 in terms of Fig. 2) have

Nets for Several Medial Polyhedra

<p>V</p>  <p>4 - 1, 3</p>	<p>V</p>  <p>5 - 1, 3, 1</p>	<p>VI</p>  <p>6 - 1, 4, 1</p>	<p>VII</p>  <p>7 - 1, 5, 1</p>
<p>VIII</p>  <p>8 - 2, 2, 2, 2</p>	<p>IX</p>  <p>9 - 3, 3, 3</p>	<p>X</p>  <p>10 - 1, 4, 4, 1</p>	<p>XII</p>  <p>12 - 1, 5, 5, 1</p>
<p>XIV</p>  <p>14 - 1, 6, 6, 1</p>	<p>XV</p>  <p>15 - 3, 3, 3, 3, 3</p>	<p>XVI-1</p>  <p>16 - 4 [1, 3]</p>	<p>XVI-2</p>  <p>16 - 2, 2, (2, 2, 2, 2), 2, 2</p>
<p>XX-1</p>  <p>20 - 1, 3, 3, (3), 3, 3, 1</p>	<p>XX-2</p>  <p>20 - 1, 6, 6, 6, 1</p>	<p>XXXII</p>  <p>32 - 1, 5, 5, 5, 5, 5, 1</p>	<p>XLII</p>  <p>42 - 1, 5, 5, 5, (10), 5, 5, 5, 1</p>

MICHAEL GOLDBERG, MARCH 1933

Fig. 2. Goldberg's medial polyhedra, 1933.

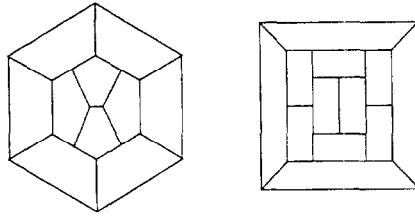


Fig. 3. Quasi-medial polyhedra $\tilde{F}_{18}(C_{2v})$ and $\tilde{F}_{22}(C_{2v})$.

greater IQ than, respectively, the regular octahedron and icosahedron: Goldberg computed that $\text{IQ}(\text{Octahedron}) < \text{IQ}(F_{12}) \simeq 0.628$ and $\text{IQ}(\text{Icosahedron}) < \text{IQ}(F_{36}(D_{6h})) \simeq 0.848$.

The following two polyhedra given in Fig. 3 are almost medial and we call them *quasi-medial* polyhedra with 18 and 22 vertices denoted by $\tilde{F}_{18}(C_{2v})$ and $\tilde{F}_{22}(C_{2v})$. While $\tilde{F}_{18}(C_{2v})$ is the edge-coalesced icosahedron [45] given in Fig. 24, $\tilde{F}_{22}(C_{2v})$ is the one-edge truncated dodecahedron mentioned on p. 274 in [57]. This polyhedron has 10 pentagonal facets which is the maximum among all simple polyhedra with 22 vertices. Both $\tilde{F}_{18}(C_{2v})$ and $\tilde{F}_{22}(C_{2v})$ and their duals are not 5-gonal. Another candidate to be quasi-medial polyhedron with 18 vertices is the one-edge truncated F_{16} [57].

1.3. Fullerenes and other extremal problems on the sphere

We recall the definition of the minimal energy potential $V_{n,k}$ on n charges lying on the unit sphere. This notion is used, for example, in stereo-chemistry, botany, virology, information theory and in the office assignment problem. With d_{pq} denoting the Euclidean distance between the point charges p and q ,

$$V_{n,k} = \begin{cases} \min_{1 \leq p < q \leq n} \sum \frac{1}{d_{pq}^k} & \text{for } k \geq 1, \\ \max_{1 \leq p < q \leq n} \sum \frac{1}{d_{pq}^k} & \text{for } k \leq -1. \end{cases}$$

Case $k = 1$. This case corresponds to the Coulombic potential (the Thomson problem). Among the configurations minimizing $V_{n,1}$ found by Edmundson [23], we have the following dual fullerenes: F_4^* , F_6^* , F_8^* , F_{10}^* , F_{16}^* , F_{18}^* , F_{20}^* , \tilde{F}_{22}^* , F_{24}^* , F_{26}^* , $F_{28}^*(T_d)$, $F_{30}^*(D_{5h})$, $C_{60}^*(I_h)$ and $C_{80}^*(D_{5h})$. Kuijlaar and Saff (see [47] and [20,21] therein) did extensive search and indicated that for $32 \leq n \leq 200$, the Voronoi domains correspond to fullerenes with only handful of exceptions.

Case $k = 2$. Among the spherical Voronoi domains of the configurations minimizing $V_{n,2}$ found by Plestenjak et al. [55], we have the following fullerenes: F_4 , F_6 , F_8 , F_{10} , F_{14} , F_{16} , $F_{18}(C_{2v})$, F_{20} , $\tilde{F}_{22}(C_{2v})$, F_{24} , F_{26} , $F_{28}(T_d)$, $F_{30}(D_{5h})$, $F_{34}(C_2)$, $F_{36}(D_{3h})$ and $F_{40}(T_d)$.

Case $k \rightarrow \infty$. This case corresponds to the Tammes problem or densest packing by hard spheres. For the thinnest covering (soft spheres) [65], the best known are:

F_4^* , F_6^* , F_8^* , F_{10}^* , F_{12}^* , F_{14}^* , F_{16}^* , F_{20}^* , $\tilde{F}_{22}^*(C_{2v})$, F_{24}^* , F_{26}^* , $F_{28}^*(T_d)$, $F_{30}^*(C_{2v})$, $F_{32}^*(D_3)$, $F_{34}^*(C_{3v})$, $F_{36}^*(D_{2d})$, $F_{40}^*(D_{5d})$, $C_{60}^*(I_h)$, $C_{140}^*(I)$, $C_{240}^*(I_h)$ and $C_{260}^*(I)$.

Case $k = -1$. The value $V_{n,-1}/\binom{n}{2}$ corresponds to the maximal average distance. For even n and d_{pq} the spherical metric, we have $\max V_{n,-1}/\binom{n}{2} = \pi/4$.

Remark 1.6. The first 8 medial polyhedra (given in Fig. 2) can be seen as networks on the sphere, that is, partitions of the sphere (into 4, ..., 10 and 12 parts) by arcs meeting at each vertex with equal angles of 120° . Together with the equipartitions of the sphere into 2 and 3 parts, they form the 10 possible partitions of this type and are the solutions of the so-called Steiner problem on the sphere [40]. All, except non-5-gonal F_{14} and F_{16} , are ℓ_1 -embeddable. One can check (see Table 13.3.1 in [37]) that all simple polyhedra with only 3-, 4- or 5-gonal facets are those 8 items and 3 ℓ_1 -polyhedra from Figs. 7 (a)–(c) of [13].

Small fullerenes also appear in the following forms:

- (i) F_{20} , $\tilde{F}_{22}(C_{2v})$, F_{24} , F_{26} and $F_{28}(D_2)$ as skeletons of central soap bubbles (see Fig. 9.13 in [25])
- (ii) F_{20} , F_{24} , F_{26} and $F_{28}(T_d)$ are the only fullerenes with *isolated hexagons*. In chemistry, their duals are called Frank–Kasper polyhedra [30].
- (iii) The vertex sets of tetrahedral F_{28} , F_{68} , C_{116} and, perhaps, C_{164} and C_{188} appear in Table 1 of [39] as putative best spherical t -designs with m points with $(m, t) = (16, 5)$, $(36, 8)$, $(60, 10)$, $(84, 12)$ and $(96, 13)$.
- (iv) In the Mosseri–Sadoc [53, 57] models similar to the one presented in Section 4.2.2, small dual fullerenes such as F_{20}^* , F_{24}^* , F_{26}^* and $F_{28}^*(T_d)$ appear as disclinations (rotational defects) with respect to the vertex figure F_{20}^* of the local icosahedral order.
- (v) Irregular F_{20} with F_{24} (also with $F_{28}(T_d)$, or F_{24} and F_{26}) fills \mathbb{R}^3 . Those space co-fillers were used in pp. 74, 136–139 and 659–664 in [70] for description of clathrate crystal structures of some ice or silicate compounds. Another space co-filler of \mathbb{R}^3 is F_{12} (item VIII of Fig. 2); this dual of the bisdisphenoid (see Table 6 and [4, 71]) embeds into $\frac{1}{2}H_8$. We also recall that the right angled hexagonal barrel F_{24} tiles the hyperbolic space H^3 — it is the fundamental polyhedron of a compact hyperbolic manifold called the Löbell space which is considered also in cosmology. The hyperbolic analogue of F_{20} and F_∞ are the following regular tilings of the Lobachevsky plane H^2 : $(5, p)$ with $p > 3$ by 5-gons and $(6, p)$ with $p > 3$ by 6-gons. Both F_{20} and F_∞ and their chamferings (defined in Section 3.4.2) are ℓ_1 -embeddable. Similarly, above two regular tilings and their chamfering are ℓ_1 -embeddable. Moreover, any regular tiling (n, p) with $1/n + 1/p < 1/2$ of the Lobachevsky plane by n -gons and its chamfering embeds into the infinite dimensional cubic lattice \mathbb{Z}_∞ for even n and into $\frac{1}{2}\mathbb{Z}_\infty$ for odd n .

Conjectures 1.3 and 1.4 present the fullerenes and their duals as a kind of best polyhedral approximation of a sphere, and the isoperimetric problem could be the underlying issue explaining, for example, the icosahedral structure of some virus capsids (see

Section 3.3). So, this paper can be considered as an investigation of ℓ_1 -embeddability of supposed best polyhedral approximation of spheres following [13,17] which are devoted to ℓ_1 -embedding of, respectively, highly regular polyhedra and infinite polyhedra (plane partitions and lattices).

2. Half-cube embeddings of fullerenes

We expected the number of embeddable fullerenes to be finite and, throughout this paper, we try to obtain the list of such fullerenes. In this section, after giving some results valid for any fullerenes and their duals, we check the ℓ_1 -status of more than 4000 small fullerenes and their duals. For example, the embeddability of all fullerenes F_n for $n < 60$ and preferable fullerenes C_n for $n < 86$ is given in Tables 2 and 3. Some infinite families are also considered. The graphs were provided by G. Brinkmann and P.W. Fowler and the ℓ_1 -status was computer checked by Pasechnik [54].

2.1. Embeddability of fullerenes and their duals

Lemma 2.1. *A fullerene F_n (and its dual F_n^*)*

- (i) *either is a ℓ_1 -rigid isometric subgraph of a half-cube,*
- (ii) *or violates a $(2k + 1)$ -gonal inequality for some integer $k \geq 2$.*

Proof. Item (i) is a direct application of Lemma 1.2. A fullerene F_n being a simple polyhedron and as its dual F_n^* has no vertex of valency 3, both do not contain K_4 and therefore are ℓ_1 -rigid (and isometric subgraph of a half-cube by the implications given at the end of Section 1.1) when ℓ_1 -embeddable. If F_n or F_n^* is not embeddable: recall, as remarked in [12], that a hypermetric but not ℓ_1 -embeddable graph has diameter 2 or 3. Then, since F_{20}^* is known to be an ℓ_1 -polyhedron and since any fullerene (and its dual except F_{20}^*) has diameter at least 4, (ii) follows. \square

While there exist 5-gonal but not 7-gonal polyhedra, for example the snub square antiprism (see [4,71]), we could not find any such fullerene. This and Lemma 2.1 lead us to the following conjecture:

Conjecture 2.2. *A fullerene F_n (and its dual F_n^*)*

- (i) *either is ℓ_1 -rigid,*
- (ii) *or violates a 5-gonal inequality.*

2.2. Embeddings of small fullerenes

Out of more than 4000 fullerenes F_n and their duals for $n < 60$, and all preferable fullerenes C_n and their duals for $n < 86$, only 4 fullerenes, $F_{20}(I_h)$, $F_{26}(D_{3h})$, $F_{44}(T)$, and $C_{80}(I_h)$, and only 4 dual fullerenes, $F_{20}^*(I_h)$, $F_{28}^*(T_d)$, $F_{36}^*(D_{6h})$ and $C_{60}^*(I_h)$, turn

Table 2
Embeddability of small fullerenes (Out of all 7916 F_n and F_n^* with $n < 60$, only 6 are ℓ_1 -embeddable)

Fullerene	ℓ_1 -embeddability of F_n	ℓ_1 -embeddability of F_n^*
$F_{20}(I_h)$	$\rightarrow \frac{1}{2}H_{10}$	$\rightarrow \frac{1}{2}H_6$
$F_{26}(D_{3h})$	$\rightarrow \frac{1}{2}H_{12}$	not 5-gonal
$F_{28}(T_d)$	not 5-gonal	$\rightarrow \frac{1}{2}H_7$
$F_{36}(D_{6h})$	not 5-gonal	$\rightarrow \frac{1}{2}H_8$
$F_{44}(T)$	$\rightarrow \frac{1}{2}H_{16}$	not 5-gonal

Table 3
Embeddability of small preferable fullerenes (Out of all 102 C_n and C_n^* with $n < 86$, only 2 are ℓ_1 -embeddable)

Fullerene	ℓ_1 -embeddability of F_n	ℓ_1 -embeddability of F_n^*
$C_{60}(I_h)$	not 5-gonal	$\rightarrow \frac{1}{2}H_{10}$
$C_{80}(I_h)$	$\rightarrow \frac{1}{2}H_{22}$	not 5-gonal

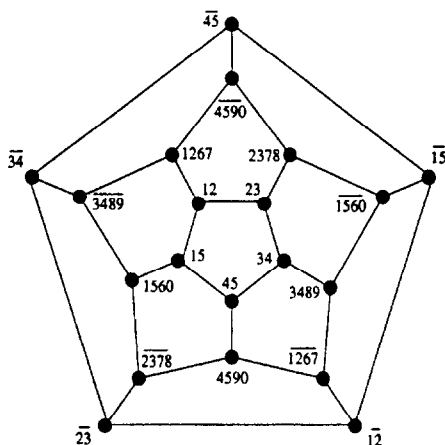


Fig. 4. Embedding of $F_{20}(I_h)$ into $\frac{1}{2}H_{10}$.

out to be ℓ_1 -embeddable (see Tables 2 and 3). The embeddings are given in detail in Figs. 4–7 where a vertex of $\frac{1}{2}H_m$ is labelled by the set $S \subset \{1, 2, \dots, m\}$ of its nonzero coordinates (\bar{S} denotes the complement of S). For example, the lower vertex v of the central pentagon of Fig. 4 is labelled by $\{4, 5\}$, i.e. $v = \{0, 0, 0, 1, 1, 0, 0, 0, 0, 0\}$ of $\frac{1}{2}H_{10}$. In Fig. 8 the edges are labelled by the symmetric difference between sets of nonzero coordinates of corresponding vertices of $\frac{1}{2}H_{22}$. The embeddings of $F_{20}(I_h)$ and its dual are trivial (see, for example, [14]) and the embeddings of $F_{26}(D_{3h})$ and $F_{28}^*(T_d)$ are given in [13].

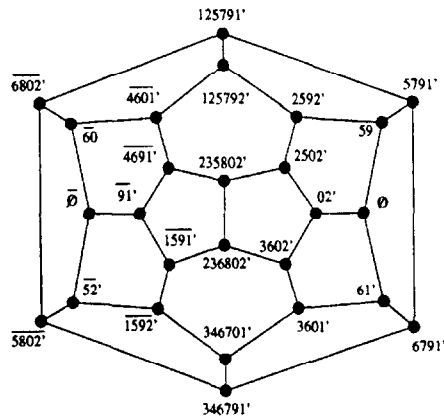


Fig. 5. Embedding of $F_{26}(D_{3h})$ into $\frac{1}{2}H_{12}$.

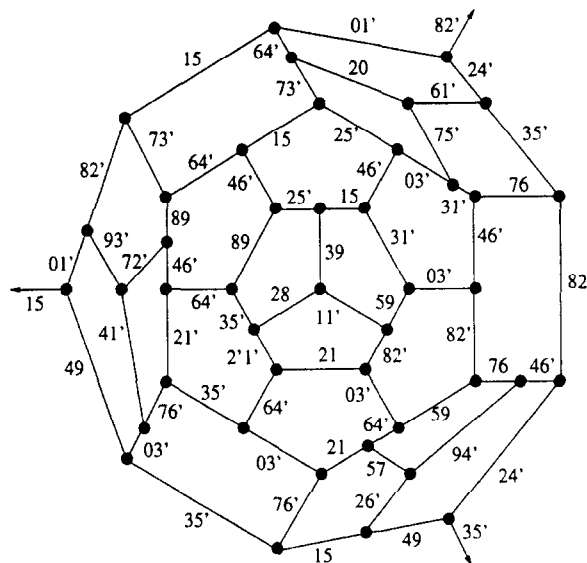


Fig. 6. Embedding of $F_{44}(T)$ into $\frac{1}{2}H_{16}$.

2.3. Infinite families of non- ℓ_1 -fullerenes

In this section we present two families of non- ℓ_1 -fullerenes based on a construction analogous to Fowler [28] carbon cylinder construction which gives preferable fullerenes. Starting from a fullerene F_n that we can separate into two *hemispheres* by cutting 5 edges (resp. 6), we insert between those hemispheres a layer of 5 hexagons (resp. 6). The obtained fullerene has $n + 10$ vertices (resp. $n + 12$) and is called a *1-layered* F_n . By inserting i layers, we get the i -layered F_n . For example, cutting anywhere F_{20} and inserting i layers, we get the i -layered dodecahedron defined as $F_{10(i+2)}(D_{5h})$ for odd i

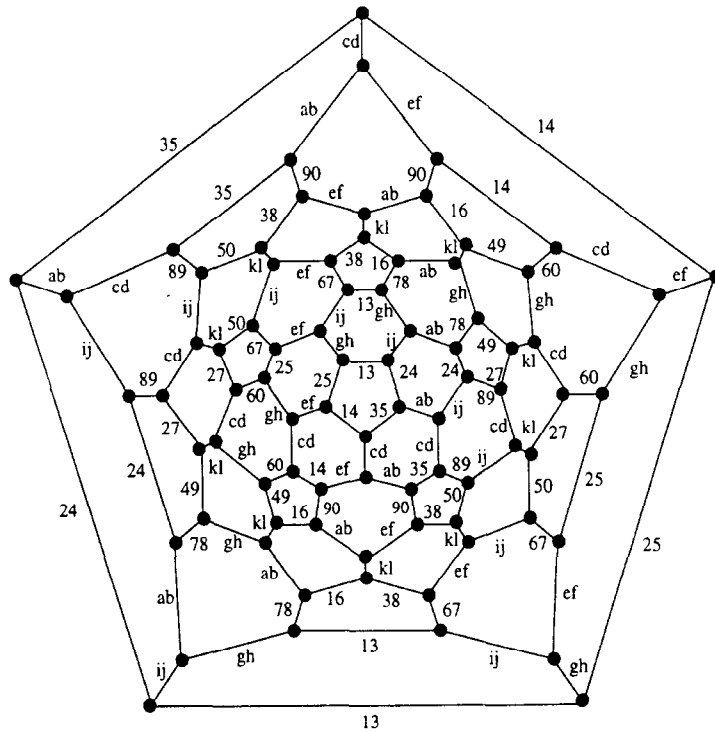


Fig. 8. Embedding of $C_{80}(I_h)$ into $\frac{1}{2}H_{22}$.

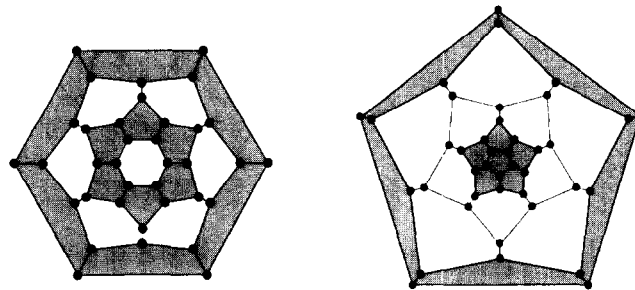


Fig. 9. $F_{36}(D_{6h}) = 1$ -layered $F_{24}(D_{6d})$ and $F_{40}(D_{5d}) = 2$ -layered dodecahedron.

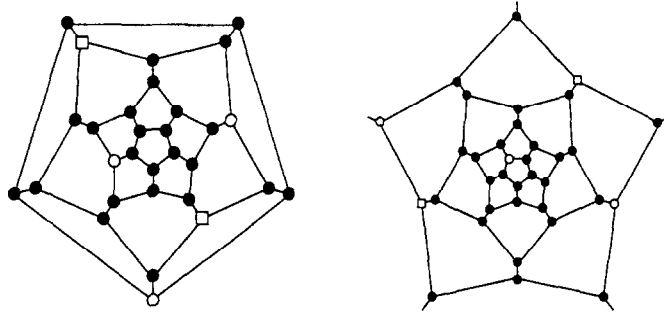
and $F_{10(i+2)}(D_{5d})$ for even i (see Fig. 9). Starting with $F_{24}(D_{6d})$ and inserting i -layers of 6 hexagons between two hemispheres made of 5 pentagons surrounding a hexagon, we get the i -layered $F_{24}(D_{6d})$: $F_{12(i+2)}(D_{6h})$ for odd i and $F_{12(i+2)}(D_{6d})$ for even i , see Fig. 9. Those two families were introduced in Table 5 of [27] as dihedral fullerenes with two caps.

Proposition 2.3. For any integer $i \geq 1$:

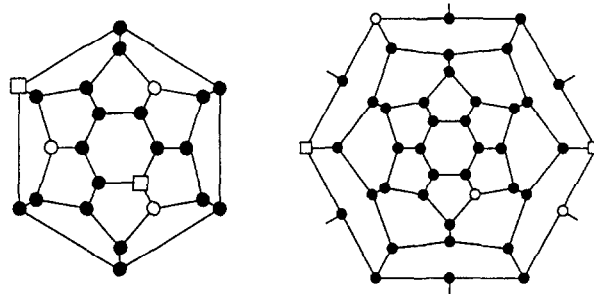
- (i) The i -layered fullerene (and its dual) $F_{10(i+2)}(D_{5h}$ or $D_{5d})$ is not ℓ_1 -embeddable, and

(ii) the i -layered fullerene (and its dual except for $i = 1$) $F_{12(i+2)}(D_{6h}$ or $D_{6d})$ is not ℓ_1 -embeddable.

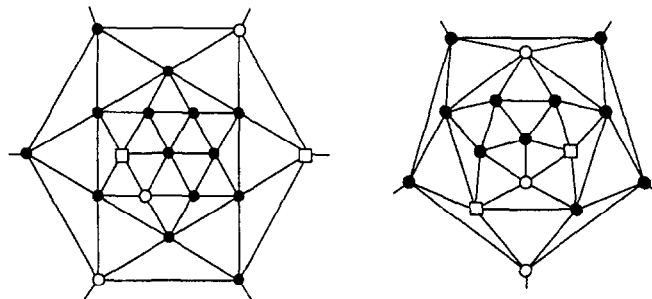
Proof. To prove that the above fullerenes are not ℓ_1 -embeddable, we simply exhibit a non-5-gonal configuration contained in their skeletons. The coefficient b_i of the violated 5-gonal inequality (see Eq. (1) of Section 1) is 0 for a black vertex, -1 for a square one, and 1 for a white circle.



The non-5-gonal configurations of i -layered $F_{10(i+2)}$ for $i = 1$ and for $i \geq 2$.



The non-5-gonal configurations of i -layered $F_{12(i+1)}$ for $i = 1$ and for $i \geq 2$.



The non-5-gonal configurations of dual i -layered $F_{12(i+1)}^*$ and $F_{10(i+1)}^*$ for $i \geq 3$. \square

Item (i) of Proposition 2.3 was given in [13] where i -layered dodecahedra were called *strained fullerenes* and were introduced as duals of 2-capped towers of $(i + 1)$ pentagonal antiprisms. Those fullerenes can be seen as somehow opposite to preferable fullerenes C_n , i.e. with many pentagons sharing a common edge. See also Propositions 3.3 and 3.6 where many other families of non- ℓ_1 -fullerenes are given.

3. Icosahedral fullerenes

To determine if ℓ_1 -embeddability is more likely to occur for fullerenes with large symmetry, we focus on *icosahedral fullerenes*, i.e. fullerenes with either the extended icosahedral group I_h of order 120 or the *proper* icosahedral group $I (=A_5)$.

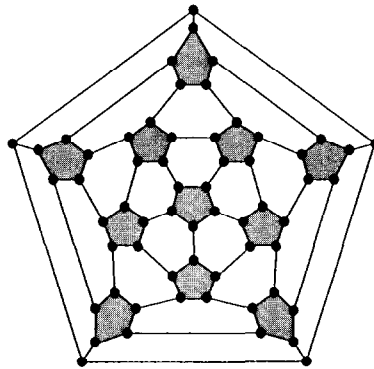
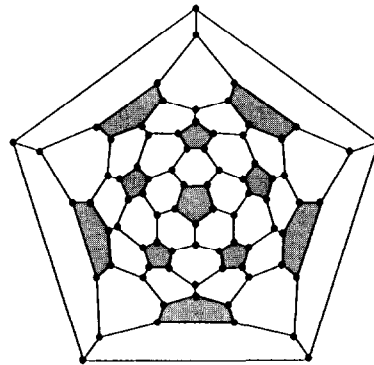
3.1. Icosahedral fullerenes

Any icosahedral fullerene $F_n(I_h)$ and $F_n(I)$ comes by folding of triangular net and satisfies $n = 20T$ with *triangulation number* $T = a^2 + ab + b^2$ for positive integers (a, b) , see [8,35]. All icosahedral fullerenes being preferable except $F_{20}(I_h)$, we denote them by $C_{20T}(I_h)$ or $C_{20T}(I)$ (abuse of notation). Moreover, $n = 60i$ if $(a - b)$ is divisible by 3, and $n = 60i + 20$ otherwise. The symmetry group of an icosahedral fullerene is I_h for $ab = 0$ or $a = b$, and I otherwise. For example, the first icosahedral fullerene $F_{20}(I_h)$ corresponds to $(a, b) = (1, 0)$; the $C_{60}(I_h)$ corresponds to $(a, b) = (1, 1)$; and the *chamfered dodecahedron* (see [34]) $C_{80}(I_h)$ corresponds to $(a, b) = (2, 0)$ (see Figs. 10 and 11, or item XLII of Fig. 2). In other words, an icosahedral fullerene is the (a, b) -generalized leapfrog of a dodecahedron (see [58]) or the $\{5+, 3\}_{a, b}$ (see [8]).

3.2. Dual icosahedral fullerenes

Call *icosadeltahedron* the duals — $C_{20T}^*(I_h)$ or $C_{20T}^*(I)$ — of an icosahedral fullerene. Those icosadeltahedra were introduced by Goldberg [35] in 1937 and (independently) by Caspar and Klug [7] in 1962 as capsids (protein coats) of some viruses. The first icosadeltahedron is the icosahedron $F_{20}^*(I_h)$; and, for $(a, b) = (1, 1)$, we have the dual buckminsterfullerene $C_{60}^*(I_h)$ which is also the pentakis dodecahedron denoted $\{3, 5+\}_{1,1}$ by Coxeter. In Fig. 12, $C_{60}^*(I_h)$ can be seen represented as omnicailed dodecahedron in *Gravitation* of Escher, which can also be seen as a small stellated dodecahedron with pentagram faces.

Remark 3.1. Another interesting family of dual fullerenes is the hypothetical boron cages (for example, see [6]). The first one, $B_{12} = F_{20}^*(I_h)$, is known experimentally: $[B_{12}H_{12}]^{2-}$. Next cases are: $B_{14} = F_{24}^*(D_{6d})$, $B_{15} = F_{26}^*(D_{3h})$, $B_{16} = F_{28}^*(T_d)$, $B_{17} =$ all three F_{30}^* , $B_{18} =$ three F_{32}^* , $B_{19} =$ three F_{34}^* , $B_{20} =$ three F_{36}^* , $B_{21} =$ three F_{38}^* , $B_{22} =$ three F_{40}^* including $F_{40}^*(T_d)$, $B_{23} =$ three F_{42}^* , $B_{24} =$ six F_{44}^* including $F_{44}^*(T)$. Next cases with tetrahedral or higher symmetry are $B_{28} = F_{52}^*(T)$, $B_{32} = C_{60}^*(I_h)$ and

Fig. 10. The $C_{60}(I_h)$ or (1,1)-dodecahedron.Fig. 11. Chamfered dodecahedron $C_{80}(I_h)$ (2,0)-dodecahedron.

$B_{92} = C_{180}^*(I_h)$. The last two are fairly stable in terms of eigenvalues of the Hückel Hamiltonian [41]. Both dual quasi-medial polyhedra $\tilde{F}_{18}^*(C_{2v})$ and $\tilde{F}_{22}^*(C_{2v})$ - see Fig. 3 — are also putative boron cages for B_{11} and B_{13} (Fig. 13).

3.3. Geodesic domes and virus capsids

In this section — which follows an approach similar to Tarnai [64] — we present icosahedral fullerenes and their duals, the icosadeltahedra, which occur as geodesic domes and as capsids of viruses. In Tables 4 and 5, the pair of integers (a, b) characterizing the triangulation number T is given for each dome or virus (see Section 3.1). *Laevo* (resp. *dextro*) denotes the icosahedral fullerene $C_{20T}(I)$ with $a > b > 0$ (resp. with $b > a > 0$).

3.3.1. Geodesic domes

Since Fuller's patent in 1954, numerous geodesic domes has been built. Some of the most famous, including the Iena test planetarium of 1922, are given in Table 4. In

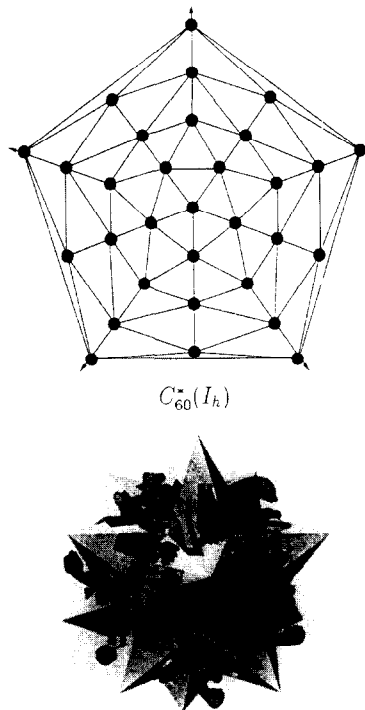


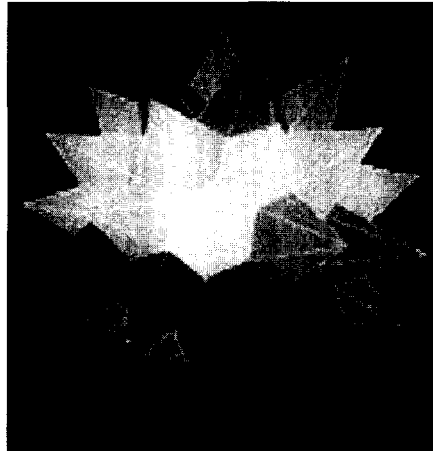
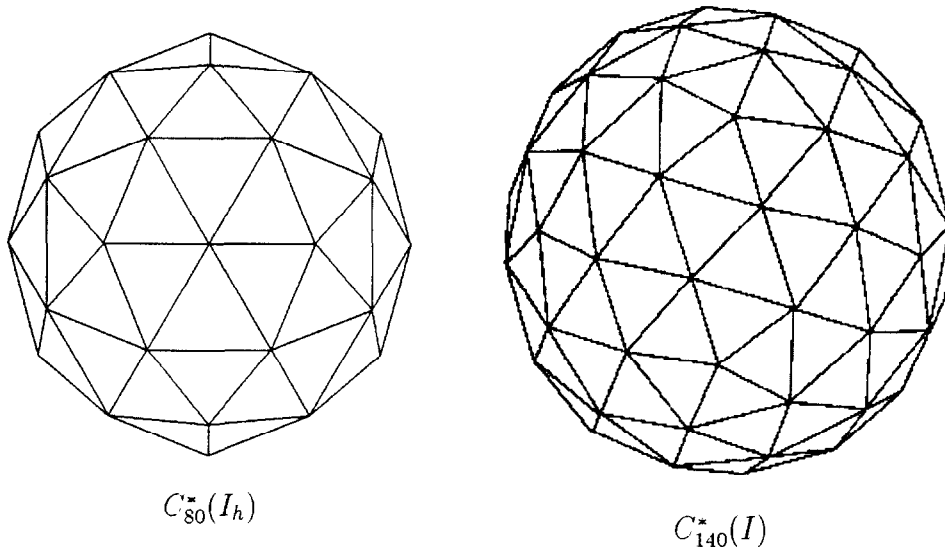
Fig. 12. Gravitation (1952) omnicapped dodecahedron.

architecture, the value $f = a + b$ is called the *frequency*; icosahedral fullerenes with $ab = 0$ are of type 1, those with $a = b$ are of type 2, and the remaining laevo and dextro fullerenes $C_{20T}(I)$ are of type 3 (types 1 and 2 correspond to *alternate* and *triacon* in Fuller terms). Note that almost all domes of Table 4 are of type 1, few are of type 2 and only one is of type 3 (and laevo).

3.3.2. Icosahedral virus capsids

A pair of icosadeltahedra (Fig. 14) of type (a, b) and (b, a) with $a > b > 0$ are mirror images of each other (or *enantiomorphous*) — for example, $C_{140}^*(I)_{\text{laevo}}$ and $C_{140}^*(I)_{\text{dextro}}$. The icosahedral structure of HIV-1 and iridovirus are proved, but the $(6, 3)$ value for the HIV-1 is still to be confirmed, and the $(10, 4)$ value for the iridovirus even if less common is also considered. Note that the majority of viruses of Table 5 are with symmetry I_h and especially of type $(a, 0)$. And among the remaining with symmetry I , only one is dextro (see [11] for a presentation of icosahedral viruses). The discovery that the majority of human virulent viruses are icosahedral recalls Plato's belief that an excess of water — whose element was supposed to be the icosahedron — is one of the main reasons for sickness (Fig. 15).

Remark 3.2. There are exactly 8 combinatorially distinct simple quasi-crystal forms, i.e. polyhedra with symmetry group I_h or I transitive on the facets (see for example



$C_{180}^*(I_h)$ as omnicailed buckminsterfullerene

Fig. 13. Three icosadeltahedra.

[33]). Namely, the icosahedron and dodecahedron embed into $\frac{1}{2}H_6$ and $\frac{1}{2}H_{10}$, respectively, and, among the six icosahedral Catalan polyhedra, the triacontahedron (= dual icosidodecahedron), the dual truncated icosahedron, and the dual truncated dodecahedron embed into H_6 , $\frac{1}{2}H_{10}$ and $\frac{1}{2}H_{26}$, respectively. The other three Catalan polyhedra, the dual rhombic icosidodecahedron, the dual truncated icosidodecahedron and the snub dodecahedron, are not 5-gonal (Fig. 16).

Table 4
Icosahedral fullerenes as geodesic domes

(a, b)	Fullerene	Geodesic dome
(1, 0)	$F_{20}^*(I_h)$	One of Salvatore Dali houses
(1, 1)	$C_{60}^*(I_h)$	Arctic Institute, Baffin Island
(2, 0)	$C_{80}^*(I_h)$	Playground toy, Kjarvalstadir, Iceland
(3, 0)	$C_{180}^*(I_h)$	Bachelor officers quarters, US Air Force, Korea
(2, 2)	$C_{240}^*(I_h)$	U.S.S. Leyte
(3, 1)	$C_{260}(I)_{laevo}$	Statue in Gagarin city, Russia
(4, 0)	$C_{320}^*(I_h)$	Geodesic Sphere, Mt. Washington, New Hampshire
(5, 0)	$C_{500}^*(I_h)$	US pavilion, Trade Fair 1956, Kabul, Afghanistan
(3, 3)	$C_{540}(I_h)$	Hafnarfjörður dome, Iceland
(6, 0)	$C_{720}^*(I_h)$	Radome, Arctic DEW
(6, 0)	$C_{720}(I_h)$	Bath at a golf course, Tokyo
(4, 4)	$C_{960}^*(I_h)$	Sky Eye radio telescope
(8, 0)	$C_{1280}^*(I_h)$	German pavilion, Osaka Expo and Accra dome, Ghana
(6, 6)	$C_{2160}(I_h)$	Children camp pavilion, Vyschod, Russia
(12, 0)	$C_{2880}(I_h)$	Children camp pavilion, Kirov, Russia
(8, 8)	$C_{3840}^*(I_h)$	Spaceship Earth, Epcot center, Florida and Lawrence, Long Island
(16, 0)	$C_{5120}^*(I_h)$	Test planetarium, Iena 1922 and US pavilion, Expo '67, Montreal
(16, 0)	$C_{5120}(I_h)$	Internal layer of US pavilion, Expo '67, Montreal
(18, 0)	$C_{6480}^*(I_h)$	Géode du Musée des Sciences, La Villette, Paris
(18, 18)	$C_{19440}(I_h)$	Union Tank Car Co., Baton Rouge, Louisiana

Table 5
Icosahedral fullerenes as virus capsids

(a, b)	Fullerene	Icosahedral virus capsid
(1, 0)	$F_{20}^*(I_h)$	Gemini virus
(1, 1)	$C_{60}^*(I_h)$	Turnip yellow mosaic virus
(2, 0)	$C_{80}^*(I_h)$	Bacteriophage ΦR
(2, 1)	$C_{140}^*(I)_{laevo}$	Rabbit papilloma virus
(1, 2)	$C_{140}^*(I)_{dextro}$	Human wart virus
(3, 1)	$C_{260}(I)_{laevo}$	Rotavirus
(4, 0)	$C_{320}^*(I_h)$	Herpes virus, varicella
(5, 0)	$C_{500}^*(I_h)$	Infectious canine hepatitis virus, adenovirus
(6, 0)	$C_{720}^*(I_h)$	HTLV-1
(6, 3)	$C_{1260}^*(I)_{laevo}$	HIV-1, usually admitted value value
(7, 7)	$C_{2940}^*(I_h)$	Iridovirus; also considered value (10, 4)

3.4. Embedding of icosahedral fullerenes

The first icosahedral fullerenes with $ab \neq 0$ and $a \neq b$, i.e. with symmetry group I , are laevo and dextro $C_{140}(I)$ with either $(a, b) = (2, 1)$ or $(1, 2)$. These fullerenes

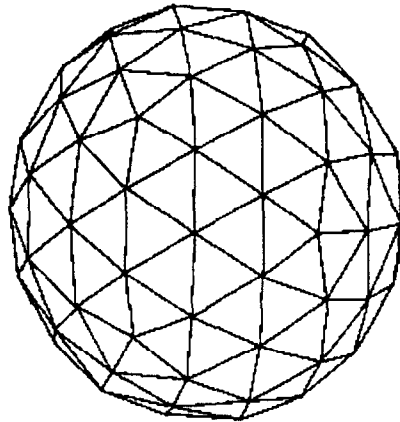


Fig. 14. Icosadeltahedron $C_{180}^*(I_h)$. Bachelor officers quarters, US Air Force, Korea.

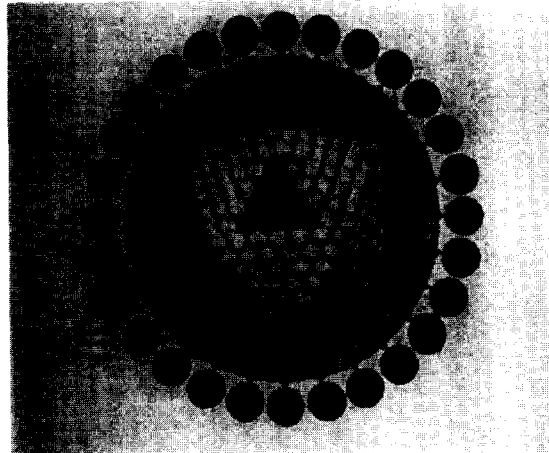


Fig. 15. The icosahedral structure $C_{720}^*(I_h)$ of the HTLV-1.

(and their duals) as well as $C_{60}(I_h)$ which is a (a, a) -fullerene with $a = 1$ arc not ℓ_1 -embeddable. We focus on icosahedral fullerenes with $b = 0$, i.e. $C_{20a^2}(I_h)$.

3.4.1. The $(a, 0)$ -dodecahedron

Since the icosahedral fullerene $C_{20a^2}(I_h)$ comes as a $(a, 0)$ -generalized leapfrog of the dodecahedron, we call it the $(a, 0)$ -dodecahedron. For example, the $(1, 0)$ -dodecahedron is the dodecahedron itself, the $(2, 0)$ -dodecahedron is the Goldberg chamfered dodecahedron $C_{80}(I_h)$ given in Fig. 11 (or item XLII of Fig. 2) and the $(3, 0)$ -dodecahedron

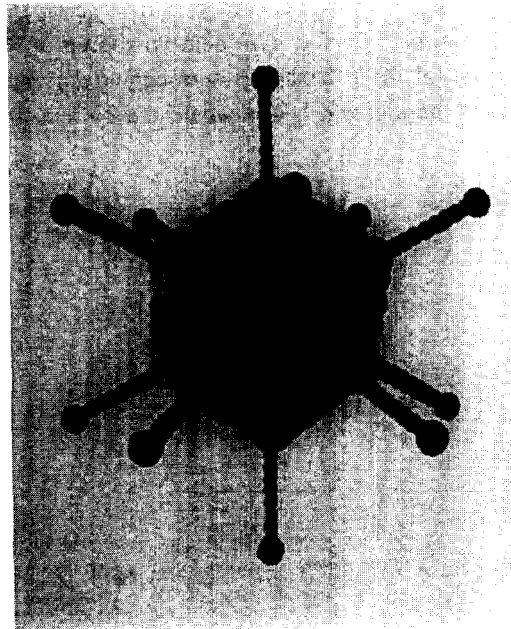


Fig. 16. Computer simulated adenovirus $C_{500}^*(I_h)$ with its spikes.

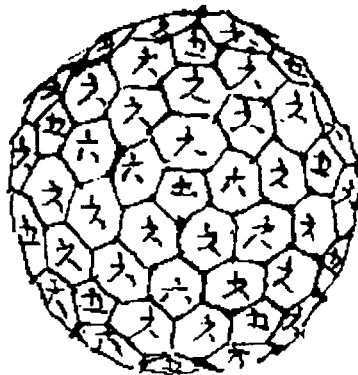
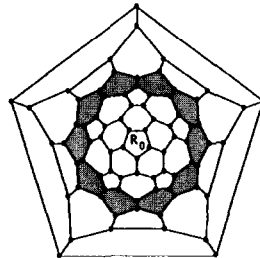


Fig. 17. The (3,0)-dodecahedron $C_{180}(I_h)$ from Sanpo-Kiriko-Shu, Edo era.

is $C_{180}(I_h)$, represented in Fig. 17, taken from *Sanpo-Kiriko-Shu* by Yasuaki Aida (1747–1817) (see Miyazaki [52]).

Proposition 3.3. *Besides the dodecahedron, the icosahedron and the chamfered dodecahedron, the $(a,0)$ -dodecahedron $C_{20a^2}(I_h)$ and its dual are not ℓ_1 -embeddable.*

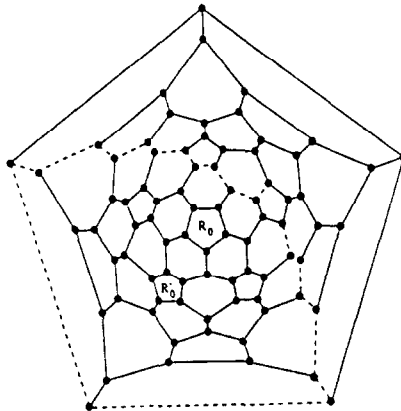
Proof. First, we recall the combinatorial structure of $C_{20a^2}(I_h)$. Identifying any pentagon with the ring R_0 , we can see $C_{20a^2}(I_h)$ being made up of $3a + 1$ rings of facets. For example, R_1 is made of the 5 hexagons surrounding R_0 and R_{3a} is the pentagon opposite to R_0 . See also the diagram below where the 10 hexagons of the ring R_3 of $C_{80}(I_h)$ are in grey.



More generally, the rings R_i and R_{3a-i} are congruent for $0 \leq i \leq 3a$. The rings containing pentagons are R_0 and R_{3a} with 1 pentagon and no hexagon and R_a and R_{2a} with 5 pentagons and $5(a-1)$ hexagons. The remaining rings R_i (without any pentagon) contain $5a$ hexagons for $a \leq i \leq 2a$ and $5i$ hexagons for $0 < i < a$ or $2a < i < 3a$. For $1 \leq i \leq 3a$, denote by C_i the set of edges separating two adjacent rings R_{i-1} and R_i , and call a hexagon of R_i *simple* (resp. *meridian*) with 2 (resp. 3) edges in C_i and 2 (resp. 1) edges in C_{i-1} ; R_0 and R_{3a} being seen as the north and south poles of $C_{20a^2}(I_h)$. Clearly, R_i contains exactly 5 meridian hexagons for $0 < i < a$ or $2a < i < 3a$ and only simple ones for $a \leq i \leq 2a$. For example, each pentagon of R_a is connected to R_0 by a chain of $(a-1)$ meridian hexagons and to two other pentagons of R_a by a chain of $(a-1)$ simple hexagons of R_a . By contracting those chains to an edge, the rings R_0, R_1, \dots, R_a collapse to the half-dodecahedron and, by doing the same for all pentagons, $C_{20a^2}(I_h)$ collapses to the dodecahedron.

To prove that $C_{20a^2}^*(I_h)$ is ℓ_1 -embeddable only for $a = 1$, we first recall some definitions. The skeleton of $C_{20a^2}(I_h)$ being of valency 3 and planar, a path entering a vertex v can exit it either by the right or the left edge. A path or circuit for which the edges can be alternatively labelled as left or right are called *alternating*. The skeleton of a polyhedron P is uniquely covered by the family of all alternating circuits where each edge belongs to at most 2 circuits. If each circuit is not self-intersecting, i.e. if each edge belongs to exactly 2 circuits, we call the family of alternating circuits *complete*. Then, if all alternating circuits of a complete family correspond to the convex cuts of the skeleton of P^* , this family gives an ℓ_1 -embedding of P^* . Namely, indexing all the circuits, each edge of P^* is labelled by the 2 indices of the circuits containing it. We first check if $C_{20a^2}^*(I_h)$ has a complete family of alternating circuits. Clearly, the circuits C_i separating rings R_{i-1} and R_i form alternating circuits for $a < i \leq 2a$; each C_i containing $10a$ edges. Since we have 6 pairs of opposite pentagons, by changing the basic pentagon R_0 we get $6a$ circuits. In the diagram below, the dotted line is the

circuit C'_4 with R_0 moved to R'_0 .



By construction, each edge of $C_{20a^2}(I_h)$ belongs to at most 2 circuits. Now, since each of those $6a$ circuits contain $10a$ edges, the family contains at least $30a^2$ edges, i.e. exactly the number of edges of $C_{20a^2}(I_h)$ — which implies that the family is complete. Moreover, for $n \leq 100$, they are only embeddable fullerene having a complete family. (For $n \leq 100$, Gunnar Brinkmann found all 24 not embeddable fullerenes having a complete family. The smallest ones are the $F_{48}(D_3)$, the $F_{56}(T_d)$ and a $F_{56}(D_{3d})$; they have a good quasi-embedding, cf. the Section 3.5). But, even if $C_{20a^2}(I_h)$ has a complete family, $C_{20a^2}^*(I_h)$ is not ℓ_1 -embeddable because those alternating circuits of $C_{20a^2}(I_h)$ do not give convex cuts of $C_{20a^2}^*(I_h)$ for $a > 1$.

Now we prove that $C_{20a^2}(I_h)$ is not embeddable for $a > 2$ by showing that its unique possible labelling do not give convex cuts. For $a > 2$, we have at least 2 rings R_k , $a < k < 2a$ which consist only of hexagons. These rings are separated by circuits C_k , $a + 1 < k < 2a$ and the edges of the ring R_k connecting vertices of the circuits C_k and C_{k+1} have the same labels. Hence, these edges determine cuts that we denote also by R_k . Actually the cuts R_k are not convex. Suppose that R_k are convex and consider two adjacent rings R_{k-1} and R_k separated by the circuit C_k . Recall that if cuts (X_1, Y_1) and (X_2, Y_2) are convex, then the intersections X_1 with X_2 , Y_1 with Y_2 and X_i with Y_j are also convex. Let $R_k = (X_k, Y_k)$ $a < k < 2a$ and X_k contains the pentagon R_0 . Then the intersection Y_{k-1} with X_k consists only of the vertices of C_k . This means that any two points of C_k are connected by a unique shortest path (going in C_k) if these points are not antipodal — while for antipodal points there are two shortest paths. Now, consider another system of rings R'_k where R'_0 is a pentagon distinct from R_0 and R_{3a} . This system determines a circuit C'_k separating two convex cuts R'_{k-1} and R'_k . This circuit C'_k has a nonempty intersection with C_k consisting of two edges x and y . These two edges are opposite in both the circuits C_k and C'_k that are even. Consider one endpoint of x and one endpoint of y . These endpoints are connected by at least two distinct shortest paths going in C_k and C'_k . This contradiction proves that the cuts R_k cannot be convex. Moreover $C_{20a^2}(I_h)$ is not 5-gonal. Actually, consider two hexagons h_k and h'_k

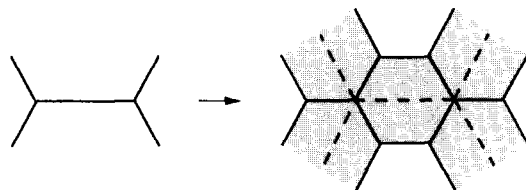


Fig. 18. The chamfering edge truncation.

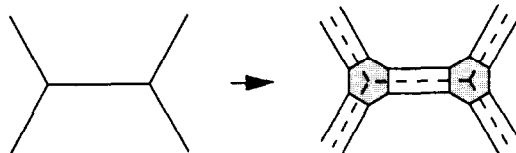


Fig. 19. Usual edge truncation.

belonging to $R_k \cap R'_k$. These hexagons contain the edges x and y with, say, $x \in h_k$, and $y \in h'_k$. Take an endpoint v of y and two opposite edges of h_k distinct from x . The endpoints of these opposite edges and v form a non 5-gonal configuration — which completes the proof. \square

Remark 3.4. The fullerenes $F_{56}(T_d)$ and $C_{140}(I_h)$ also have a complete family of circuits giving nonconvex cuts in their duals which, therefore, are not ℓ_1 -embeddable. Actually, all known ℓ_1 -fullerenes are somehow exceptional. Besides the dodecahedron $F_{20}(I_h)$ which is exceptional in many ways, $F_{26}(D_{3h})$ and $F_{80}(I_h)$ have induced subgraphs which are not 5-gonal but both are not isometric, $F_{26}(D_{3h})$ and $F_{44}(T)$ admit nonconvex alternating cuts, i.e. some — only one for $F_{44}(T)$ — convex cuts defining their embedding are non-alternating.

3.4.2. Chamfered dodecahedron

We now consider a special case of the $(a,0)$ -dodecahedron where $a = 2^t$ for an integer t . Since $C_{80}(I_h)$ was named the *chamfered dodecahedron* by Goldberg in [34], we call t -*chamfered dodecahedron* the $(2^t, 0)$ -dodecahedron $C_{20 \cdot 2^{2t}}(I_h)$. Clearly, the 0-chamfered dodecahedron is the dodecahedron itself, the 1-chamfered dodecahedron is the chamfered dodecahedron and the 2- and 4-chamfered dodecahedra are, respectively, $C_{320}(I_h)$ and $C_{5120}(I_h)$ — the dual of Mt. Washington and of Iena planetarium presented in Table 4. Those t -chamfered dodecahedra are the result of the (t) -times edge truncation illustrated by Fig. 18, which was also given in [27] as the *quadrupling transformation* for fullerenes. The chamfering — also used by Grünbaum [37, p. 263] — as well as the leapfrog operation were introduced in 1891 by Eberhard in [21, p. 180] as Π_2 and Π_1 constructions, respectively.

For any polyhedron P , denote $\text{Cham}_t(P)$ the t -times chamfered P . Each vertex v of P with valency k_v will create k_v new vertices in $\text{Cham}_1(P)$ and each edge of P will create

a hexagon. So, the f -vector of the chamfering of a polyhedron P with constant vertex incidence k is $f(\text{Cham}_1(P)) = ((k+1)f_0(P), k f_0(P) + 2f_1(P), f_1(P) + f_2(P))$ and the p -vector is preserved except $p_6(\text{Cham}_1(P)) = p_6(P) + f_1(P)$. For a fullerene, the chamfering corresponds to a (2,0)-leapfrog transform and we have $\text{Cham}_1(F_n(S_g)) = C_{4n}(S_g)$ where S_g is the symmetry group of F_n . We also recall in Fig. 19 the well-known edge truncation given in Ch. 10 of Loeb [49].

Proposition 3.5. *With the definition of alternating circuits given in the proof of Proposition 3.3, two necessary conditions for the ℓ_1 -embeddability of the t -chamfered fullerene $(2^t, 0)$ - F_n are:*

- (i) F_n is ℓ_1 -embeddable and
- (ii) the family of alternating circuits of F_n is complete.

Proof. By induction, it is enough to prove it for the 1-chamfering. Let us denote by $E(F_n)$ the set of edges of F_n and by $\text{Cham}(F_n)$ the chamfering of F_n . We have $E(\text{Cham}(F_n)) = E_1(\text{Cham}(F_n)) \cup E_2(\text{Cham}(F_n))$ where there is a one-to-one correspondence between pairs of parallel *old* edges of new hexagons of $E_1(\text{Cham}(F_n))$ and the edges $E(F_n)$, and where the *new* edges $E_2(\text{Cham}(F_n))$ are the edges of $\text{Cham}(F_n)$ shared by the new hexagons of $\text{Cham}(F_n)$. Now, assume that F_n is ℓ_1 -embeddable. Using the same terminology as for the proof of Proposition 3.3, the ℓ_1 -embeddability into $\frac{1}{2}H_m$ of F_n means that we can label its edges by pairs: (i, j) $1 \leq i < j \leq m$ such that equivalent edges are labelled by the same pair (see, for example, Fig. 8). Then, since by construction the chamfering preserves the equivalence relation, the ℓ_1 -embeddability of $\text{Cham}(F_n)$ implies the ℓ_1 -embeddability of F_n (same labeling for $E_1(\text{Cham}(F_n))$ and for $E(F_n)$). To prove (ii), we notice that edges of $E_2(\text{Cham}(F_n))$ are partitioned into equivalence classes not intersecting with equivalence classes of $E_1(\text{Cham}(F_n))$, moreover those equivalence classes of $E_2(\text{Cham}(F_n))$ are in one-to-one correspondence with the alternating circuits of F_n . Now, if $\text{Cham}(F_n)$ is ℓ_1 -embeddable, the equivalence classes of $E_2(\text{Cham}(F_n))$ are precisely the convex cuts of $\text{Cham}(F_n)$ and the corresponding alternating circuits of F_n form the complete family of alternating circuits. Which completes the proof. \square

Proposition 3.6. *Applying item (i) of Proposition 3.5, for any integer $\geq t$, the following families of fullerenes are not ℓ_1 -embeddable: $C_{60 \cdot 2^{2t}}(I_h)$, $C_{140 \cdot 2^{2t}}(I)$, $C_{28 \cdot 2^{2t}}(T_d)$, $C_{56 \cdot 2^{2t}}(T_d)$ and $C_{76 \cdot 2^{2t}}(T_d)$. By item (ii), for any integer $\geq t$, the t -chamfered $F_{26}(D_{3h}) = C_{26 \cdot 2^{2t}}(D_{3h})$ is not ℓ_1 -embeddable.*

Remark 3.7. Taking the pentakis (capping of all pentagons) of dodecahedron, icosidodecahedron (7), snub dodecahedron (18), pentagonal orthobirotunda (54) (also called anti-icosidodecahedron) gyroelongated pentagonal birotunda (68), we obtain $C_{60}^*(I_h)$, $C_{80}^*(I_h)$, $C_{140}^*(I)$, $C_{80}^*(D_{5h})$ (i.e. the dual twisted $\text{Cham}(F_{20}(I_h))$) and a C_{100}^* . The 3 regular-faced polyhedra numbers (7), (54) and (68) [4] come from the pentagonal rotunda M_9 ; precisely, (7) = $M_9 + \bar{M}_9$, (54) = $2 M_9$ and (68) = $M_9 + \text{Antiprism}_{10} + M_9$.

Those 3 polyhedra are not 5-gonal, the snub dodecahedron is ℓ_1 -rigid embeddable into $\frac{1}{2}H_{15}$; $C_{80}^*(I_h)$, $C_{140}^*(I)$, $C_{80}^*(D_{5h})$ and C_{100}^* are not 5-gonal.

3.4.3. Edge truncations

The Loeb edge truncation of the 5 Platonic solids gives 3 Archimedean zonohedra. Namely, by this edge truncation the tetrahedron becomes the truncated octahedron, both octahedron and cube become the truncated cuboctahedron and both icosahedron and dodecahedron become the truncated icosidodecahedron. For the same 5 Platonic solids, the chamfered tetrahedron is the dual 4-capped octahedron (the capped facets being pairwise nonadjacent), the chamfered icosahedron (resp. dodecahedron) is the dual triakis (resp. pentakis) icosidodecahedron and the chamfered cube (resp. octahedron) is the dual tetrakis (resp. triakis) cuboctahedron. Actually, any zonohedron being embeddable into a cube, the chamfered cube, which is a simple zonohedron, embeds into H_7 ; its generators are $e_1, e_2, e_3, (e_1 \pm e_2)$ and $(e_1 \pm e_3)$. On the other hand, the chamfering of the Prism_6 and the rhombic dodecahedron, which are both zonohedra, gives polyhedra which are neither zonohedra nor ℓ_1 -embeddable. The chamfered cube provides the following nice link between the dodecahedron and the rhombic dodecahedron (dually, the transition between the icosahedron and the cuboctahedron is known in chemistry, see [70, p. 146]). The chamfered cube is, on the one hand, partially (on the six 4-valent vertices) the vertex truncation of the rhombic dodecahedron and, on the other hand, is partially (on the six edges linked pairwise by no less than two edges) the Loeb edge truncation of the dodecahedron.

Remark 3.8. The proof of Proposition 3.5 never considers that F_n is a fullerene — it holds for the chamfering of any polyhedron. The tetrahedron is an example of polyhedron for which the chamfering is not ℓ_1 -embeddable while satisfying the conditions of Proposition 3.5.

Proposition 3.9. *Among the Platonic solids, their chamferings and the duals of their chamferings, only the tetrahedron, the octahedron, the icosahedron, the cube and its chamfering, the dodecahedron and its chamfering and dual chamfered tetrahedron are ℓ_1 -embeddable. Moreover, they embed into $\frac{1}{2}H_{2\delta}$ where δ denotes the diameter of the polyhedron except the tetrahedron — which is $\frac{1}{2}H_3$ — and the dual chamfered tetrahedron which embeds into $\frac{1}{2}H_8$ while its diameter is 3. Recall that all known embeddable fullerenes (and all embeddable dual fullerenes except $F_{28}^*(T_d) \rightarrow \frac{1}{2}H_7$ while $\delta(F_{28}^*(T_d)) = 4$) embed into $\frac{1}{2}H_{2\delta}$. The $(a, 0)$ -cube and its dual are not ℓ_1 -embeddable for $a \geq 3$.*

3.5. Quasi-embeddings of C_{60} and $F_{60}^*(C_s)$,

Quasi- C_{60} . Even if C_{60} is not ℓ_1 -embeddable, we still can quasi-embed it into $\frac{1}{2}H_{20}$ in the following sense. We consider a relaxation of the notion of ℓ_1 -embedding which

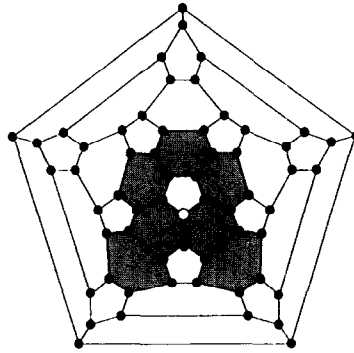
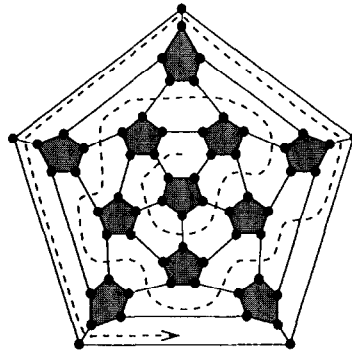
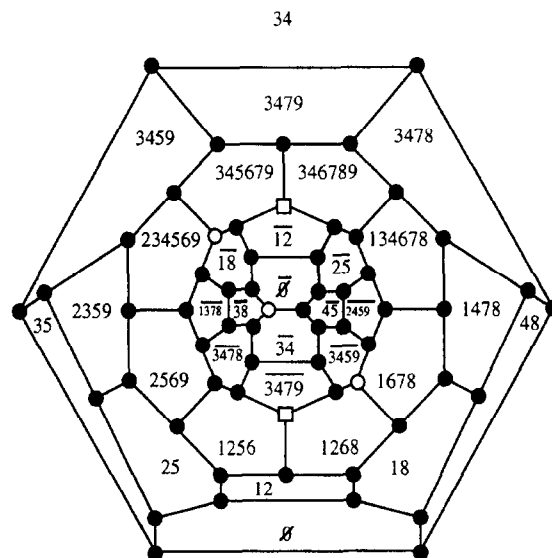


Fig. 20. Embedding up to distance 7 of $C_{60}(I_h)$ into $\frac{1}{2}H_{20}$.

allows us to find the ℓ_1 -metric somehow *closest* to the C_{60} . We say that a metric d is t -embeddable if there is an ℓ_1 -embeddable metric d' such that $d'_{i,j} = \min(d_{i,j}, t)$. This notion was introduced in [16] where it was shown that the polynomial algorithm given there for the recognition of the ℓ_1 -graph can be extended to the recognition of t -embeddable graphs. In particular, a unique 3-embedding into $\frac{1}{2}H_{20}$ of C_{60} , called quasi- C_{60} , which is also a 7-embedding, is given there. Moreover, quasi- C_{60} is an ℓ_1 -rigid (but not graphic) metric. There are at least two 2-embeddings of C_{60} . Actually any simple polyhedron with m facets admits a 2-embedding into $\frac{1}{2}H_m$ where each vertex is associated to the 3 facets containing it. Therefore any F_{60} is 2-embeddable into $\frac{1}{2}H_{32}$. The Fig. 20 illustrates the 7-embedding of C_{60} . The construction is the following: to each of the 20 hexagons we can associate a coordinate of \mathbb{R}^{20} . Then a vertex v (for example the white atom of Fig. 20) is mapped to the vertex $\phi(v)$ of the odd half-cube $\frac{1}{2}\overline{H}_{20}$ whose non-zero coordinates correspond to the 7 hexagons of C_{60} containing a vertex with distance to v less than 3 (the 7 grey hexagons of Fig. 20). This give us a 7-embedding of C_{60} into the odd half-cube $\frac{1}{2}\overline{H}_{20}$, and by adding modulo 2 any $\phi(v)$ to all the 60 vertices of quasi- C_{60} we get a 7-embedding into $\frac{1}{2}H_{20}$. All distances of length 8 and 9 in C_{60} became 7 in quasi- C_{60} (recall that C_{60} has diameter 9). It could be interesting to compare the automorphism group of quasi- C_{60} (i.e. all the permutations of the 20 coordinates indexed by the 20 hexagons of C_{60} which preserve quasi- C_{60}) with the one of C_{60} , which is the icosahedral group A_5 . Fig. 21 illustrates one automorphism of quasi- C_{60} we found: the reversing of the spiral Hamiltonian path on the 20 hexagons of C_{60} .

Quasi- $F_{60}^(C_s)_r$.* The dual of $F_{60}(C_s)_r$, considered in Section 2.2, admits a 4-embedding into $\frac{1}{2}H_{10}$. More precisely, $F_{60}^*(C_s)_r$ has diameter 5 and all distances are preserved except between 4 opposite pentagons: $(\overline{38}, \overline{48})$, $(\overline{1378}, \overline{1478})$, $(\overline{45}, \overline{35})$ and $(\overline{2459}, \overline{2359})$. Instead of 5, those distances became 4 in $\frac{1}{2}H_{10}$. See Fig. 22, where the vertices of $F_{60}^*(C_s)_r$ are labelled as facets of $F_{60}(C_s)_r$, and where a non 5-gonal configuration of $F_{60}(C_s)_r$ is given.

Fig. 21. The spiral Hamiltonian automorphism of quasi- C_{60} .Fig. 22. The 4-embedding $F_{60}^*(C_s)_r$ into $\frac{1}{2}H_{10}$ and a non-5-gonal configuration of $F_{60}(C_s)_r$.

4. Other chemically relevant polyhedra and fullerene analogues

4.1. Coordination polyhedra, metallopolyhedra and Bravais lattices

4.1.1. Coordination polyhedra and metallopolyhedra

According to Wells [70], the chemical crystal structure is usually described by (a) the *coordination polyhedron*: the convex hull of anions forming the group of nearest neighbours of each metal ion; or (b) the *domain of atom* (Voronoi–Dirichlet polyhedron). Coordination polyhedra are arrangements of nearest neighbours in crystals, molecules and ions. More precisely, as defined by Frank and Kasper in [30], a *coordination polyhedron* is the convex hull of the mirror images of the centre of a

Table 6
Embeddability of some of the most frequent chemical polyhedra

Polyhedron (n° as regular-faced)	ℓ_1 -embeddability	Example
<i>Tetrahedron</i> (1)	$\rightarrow \frac{1}{2}H_3$	$Rh_4(CO)_{12}$
<i>Octahedron</i> (2)	$\rightarrow \frac{1}{2}H_4$	$[Os_6(CO_{18})]^{2-}$
<i>Cube</i> (3)	$\rightarrow H_3$	$CsCl$
<i>Icosahedron</i> (4)	$\rightarrow \frac{1}{2}H_6$	$[Mo_{12}O_{30}(CeO_{12})]^{8-}$
<i>Cuboctahedron</i> (6)	not 5-gonal	$[Mo_{12}O_{36}(SiO_4)]^{4-}$
<i>Truncated tetrahedron</i> (8)	not 5-gonal	$[Mo_{12}(HOAsO_3)_4O_{34}]^{4-}$
<i>Rhombicuboctahedron</i> (13)	$\rightarrow \frac{1}{2}H_{10}$	$[V_{18}O_{42}(SO_4)]^{8-}$
<i>Triangular prism</i> (19)	$\rightarrow \frac{1}{2}H_5$	$[Rh_6C(CO)_{15}]^{2-}$
<i>Square antiprism</i> (20)	$\rightarrow \frac{1}{2}H_5$	$[Co_8C(CO)_{18}]^{2-}$
<i>Square pyramid</i> (21)	$\rightarrow \frac{1}{2}H_4$	$Fe_5C(CO)_{15}$
<i>Triangular cupola</i> (23)	not 5-gonal	$[W_9O_{30}(PO_4)]^{9-}$
<i>Gyroelongated square pyramid</i> (30)	extreme hypermetric	$[Co_9Si(CO)_{21}]^{2-}$
<i>Triangular bipyramid</i> (32)	$\rightarrow \frac{1}{2}H_4$	$Os_5(CO)_{16}$
<i>Pentagonal bipyramid</i> (33)	not 5-gonal	K_3ZrF_7
<i>Elongated square bipyramid</i> (35)	$\rightarrow \frac{1}{2}H_6$	$[W_{10}O_{32}]^{4-}$
<i>Gyroelongated square bipyramid</i> (37)	extreme hypermetric	$[V_{10}O_{26}]^{4-}$
<i>Triangular orthobicupola</i> (47)	not 5-gonal	$[W_{12}O_{36}(SiO_4)]^{4-}$
<i>Square gyrobicupola</i> (49)	not 5-gonal	$[V_{10}O_{26}]^{4-}$
<i>Elongated triangular bicupola</i> (55)	not 5-gonal	$\alpha\text{-}[W_{18}P_2O_{62}]^{6-}$
<i>Elongated triangular gyrobicupola</i> (56)	not 5-gonal	$\beta\text{-}[W_{18}P_2O_{62}]^{6-}$
<i>Twisted rhombicuboctahedron</i> (57)	not 5-gonal	$[H_4V_{18}O_{42}(Br)]^{9-}$
<i>Elongated pentagonal bicupola</i> (58)	not 5-gonal	$[W_{30}P_5O_{110}(Na)]^{14-}$
<i>Augmented triangular prism</i> (69)	$\rightarrow \frac{1}{2}H_5$	$Na_5Zr_2F_{13}$
<i>Biaugmented triangular prism</i> (70)	$\rightarrow \frac{1}{2}H_5$	$N_2H_6(ZrF_6)$
<i>Triaugmented triangular prism</i> (71)	extreme hypermetric	$Eu(OH)_3$
<i>Bisdisphenoid</i> (104)	not 5-gonal	K_4ZrF_8
<i>Octahedron + Pyramid₃</i>	$\rightarrow \frac{1}{2}H_5$	$[Ru_7(CO)_{16}]^{3-}$
<i>Octahedron + 2 Pyramid₃</i>	$\rightarrow \frac{1}{2}H_6$	$[Os_8(CO)_{22}]^{2-}$
<i>Tetrahedron + 2 Pyramid₃</i>	$\rightarrow \frac{1}{2}H_5$	$[Os_6(CO)_{18}]^{2-}$
<i>Edge-coalesced icosahedron</i>	extreme hypermetric	$[B_{11}H_{11}]^{2-}$

Voronoi–Dirichlet domain in each of its faces. Note that the coordination polyhedron is, in general, not dual to the Voronoi–Dirichlet domain, and different from the contact polytope of sphere packing. For example, while the Voronoi–Dirichlet polyhedron of a point of the lattice A_3^* (body-centred cubic lattice) is the truncated octahedron, its coordination polyhedron is the rhombic dodecahedron. In addition to some frequent coordination polyhedra, the ℓ_1 -status of some metallocopolyhedra (convex hull of atoms of metallic cluster) or metal and oxygen polyhedra (see [10,45,67,70]) are given in Table 6. The names and the number (as regular-faced polyhedra) are taken from the list of such 112 polyhedra given in [4,71]. For example, see Fig. 23 where the embedding of the rhombicuboctahedron (13) and the non-5-gonality of the twisted one (57) are given.

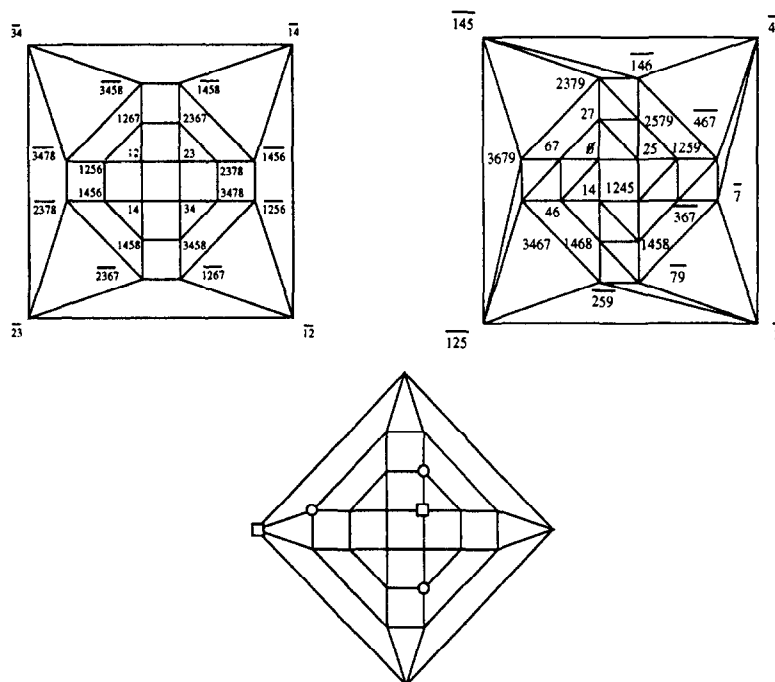


Fig. 23. The rhombicuboctahedron embeds into $\frac{1}{2}H_{10}$, the snub cube into $\frac{1}{2}H_9$ and the twisted rhombicuboctahedron is not 5-gonal.

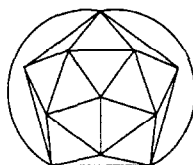


Fig. 24. The edge-coalesced icosahedron.

Remark 4.1. The regular-faced polyhedra from Table 6 with numbers 1, 2, 4, 32, 33, 37, 71 and 104 are the 8 convex deltahedra with regular facets and with n vertices $4 \leq n \leq 12$, $n \neq 11$. Those deltahedra are dual of the first 8 medial polyhedra F_n given in Fig. 2 with $n = 4, 8, 20, 6, 10, 16, 14$ and 12. The edge-coalesced icosahedron is a deltahedron with 11 vertices but with irregular facets. By deleting one of the curved edges of Fig. 24 we obtain the regular-faced augmented sphenocorona (107) with one facet a square. Both are *extreme hypermetric* [12,15] and, together with the 1-capped *Antiprism*₅, can be seen as quasi-deltahedra with 11 vertices.

Remark 4.2. The last three ℓ_1 -embeddable polyhedra of Table 6 are capped or 2-capped Platonic solids. More generally, i -capped tetrahedron $\rightarrow \frac{1}{2}H_{3+i}$ for $1 \leq i \leq 4$, i -capped octahedron $\rightarrow \frac{1}{2}H_{4+i}$ for $1 \leq i \leq 8$, i -capped cube $\rightarrow \frac{1}{2}H_6$ for $1 \leq i \leq 2$, or

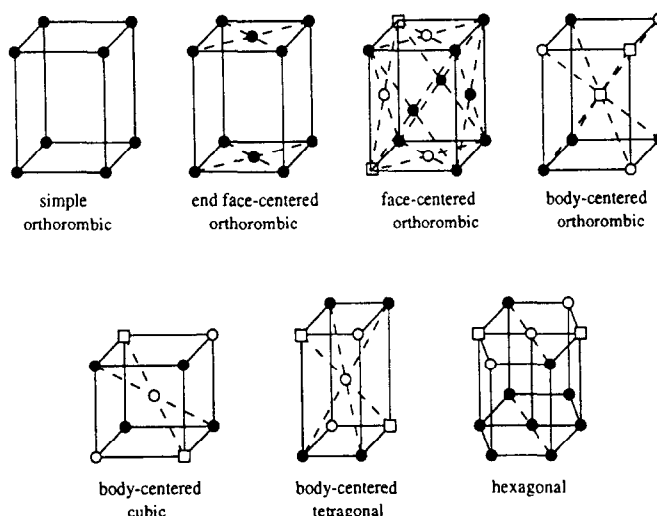


Fig. 25. The 7 graphs of the 14 unit cells of Bravais lattices.

$i = 3$ without opposite capping, and i -capped cube is not 5-gonal for $4 \leq i \leq 6$ or $i = 3$ with opposite capping. The 2-capped cube with opposite capping and the 6-capped cube appear as, respectively, the second and third graph of Fig. 25. One can easily see that, for a simplicial polyhedron P with m facets satisfying $P \rightarrow \frac{1}{2}H_n$, the omnicaapping (sometimes called 2D-subdivision in topology) of P embeds into $\frac{1}{2}H_{n+m}$. For example, the i -times omnicaapped $C_{60}^*(I_h)$ embeds into $\frac{1}{2}H_{10(3^{i+1}-2)}$. The cuboctahedron and the triangular orthobicupola are the coordination polyhedra of, respectively, the face-centered lattice and the hexagonal close packing; their duals are space fillers with the dual of the second one being non-5-gonal.

4.1.2. Bravais lattices

The 14 Bravais lattices are divided into 7 crystal systems (see, e.g. [68]). It is easy to see that their unit cells form 7 graphs represented in Fig. 25. The first two embed into $\frac{1}{2}H_6$ and the next five are not 5-gonal. As in Fig. 23 the coefficients of a violated 5-gonal inequality are, respectively, 0 for a black vertex, -1 for a square one, and 1 for a white circle.

4.2. Fullerene analogues

4.2.1. Fullerene square and triangular analogues

A square (versus pentagon) analogue of a fullerene is a simple polyhedron \diamond_n for which the n vertices are arranged in six 4-gons and $(n/2 - 4)$ hexagons (and $\frac{3}{2}n$ edges). Square fullerenes \diamond_n can be constructed for all even $n \geq 8$ except $n = 10$ (see [37, p. 271]). There are 1, 0, 1, 1, 1, 1, 3, 1, 3, 3, 3, 2, 8, 3, 7, 7, 7, 5, 14 square fullerenes \diamond_{2k} for $4 \leq k \leq 22$ [18]. The cube and the hexagonal prism are the unique square fullerenes

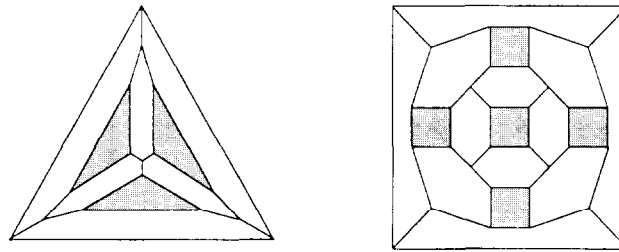


Fig. 26. Chamfered tetrahedron Δ_{16} and chamfered cube \diamond_{32} .

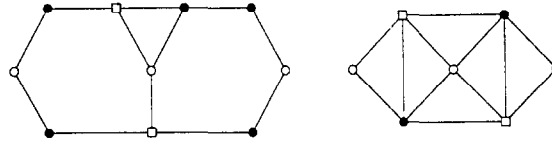
\diamond_8 and \diamond_{12} . Besides the $(a, 0)$ -cube for $a > 0$, examples of *preferable* polyhedra, i.e. without pair of 4-gons sharing a common edge, are duals tetrakis P , where P is the cube, cuboctahedron, triangular orthobicupola, gyroelongated triangular bicupola and snub cube with, respectively, 24, 32, 32, 44 and 56 vertices. The first 2 are the truncated octahedron and the chamfered cube and let us call the third one the *twisted chamfered cube*; they respectively embed in $\frac{1}{2}H_6$, $\frac{1}{2}H_7$ and $\frac{1}{2}H_7$. Similarly to the dual pentakis snub dodecahedron $C_{140}(I)$ and its dual, the last one, i.e., the dual tetrakis snub cube $\diamond_{56}(O)$ and its dual are not 5-gonal. As a regular-faced polyhedron [4, 71] the gyroelongated triangular bicupola has number (64) and equals $M_4 + \text{Antiprism}_6 + M_4$, the cuboctahedron (6) = $M_4 + \bar{M}_4$ and the triangular orthobicupola (47) = $2M_4$ (also called anticuboctahedron) where M_4 is the triangular cupola. Being bipartite, square fullerenes \diamond_n satisfy an analogue of Conjecture 2.2, i.e. \diamond_n either embeds into a hypercube or violates a 5-gonal inequality.

Another analogue is the *triangular* (versus pentagon) fullerene Δ_n , i.e. a simple polyhedron for which the n vertices are arranged in 4 triangles and $(n/2 - 2)$ hexagons (and $\frac{3}{2}n$ edges). Triangular fullerenes Δ_n can be constructed for all $n \equiv 0 \pmod{4}$ except $n = 8$ (see [37, p. 271]). There are 1, 0, 1, 2, 1, 2, 2 triangular fullerenes Δ_{4k} for $1 \leq k \leq 7$ [18]. Except the tetrahedron, all triangular fullerenes are *preferable* and have at least 4 hexagons. Examples of such polyhedra are the tetrahedron Δ_4 , the truncated one Δ_{12} and the chamfered one Δ_{16} . Similarly to classical fullerenes F_n , their square and triangular analogues are closed under leapfrog and chamfering operations (Fig. 26).

Proposition 4.3.

- (i) All known ℓ_1 - \diamond_n are: the cube, the Prism_6 , the truncated octahedron, the chamfered cube and the twisted one. While the last one is not centrally symmetric, the 4 others are zonohedra with the chamfered cube being not space-filling.
- (ii) The octahedron is the unique ℓ_1 -embeddable dual square fullerene \diamond_n^* .
- (iii) The tetrahedron is the unique ℓ_1 -embeddable triangular fullerene Δ_n .
- (iv) Besides the tetrahedron, all known ℓ_1 - Δ_n^* are: the triakis tetrahedron $\Delta_{12}^* \rightarrow \frac{1}{2}H_7$, the duals of the chamfered tetrahedron and the twisted one, i.e. both $\Delta_{16}^* \rightarrow \frac{1}{2}H_8$, the 4-capped on disjoint facets icosahedron $\Delta_{28}^* \rightarrow \frac{1}{2}H_{10}$ and the dual of the leapfrog of the triakis tetrahedron $\Delta_{36}^*(T_d) \rightarrow \frac{1}{2}H_{11}$.

Proof. As in Proposition 2.3, to prove that above fullerenes are not ℓ_1 -embeddable, we simply exhibit a non-5-gonal configuration contained in their skeletons. The coefficients b_i of the violated 5-gonal inequality (see Eq. (1) of Section 1) are, respectively, 0 for a black vertex, -1 for a square one, and 1 for a white circle.



The non-5-gonal configurations of Δ_n and \diamond_n^* .

4.2.2. Mosseri-Sadoc model: 4-dimensional fullerenes?

Mosseri and Sadoc (see, e.g. [53,57]) developed models of non crystalline solids. They use four-dimensional polytopes derived by iterative subdivision of the following icosahedron and dodecahedron analogue: the regular 4-dimensional 600-cell $\{3, 3, 5\}$ and its dual the regular 120-cell $\{5, 3, 3\}$ made of respectively 600 tetrahedra and 120 dodecahedra. Such packings do not fill \mathbb{R}^3 , but a suitable map to \mathbb{R}^3 minimizing energy provides realistic amorphous structures.

One example is the following icosadeltahedron analogue: starting from $G^0 = \{3, 3, 5\}$, G^1 is obtained by adding the mid-point of all edges of G^0 . That is, each tetrahedral facet of $\{3, 3, 5\}$ is divided into 4 tetrahedra and 1 octahedron. So, in the same way as in \mathbb{R}^3 , each triangular facet of the icosahedron $\{3, 5\}$ is covered by a portion of the hexagonal lattice A_2 , each tetrahedral facet of the 600-cell $\{3, 3, 5\}$ is covered by a portion of the face-centred cubic lattice A_3 . Iteratively, G^t is obtained from G^{t-1} by adding the mid-point of all edges of G^{t-1} , each octahedron being divided into 8 tetrahedra and 6 octahedra. Therefore, G^t has a_t tetrahedral facets and b_t octahedral facets where $a_t = 4a_{t-1} + 8b_{t-1}$, $b_t = a_{t-1} + 6b_{t-1}$, $a_0 = 600$ and $b_0 = 0$. While the lattice A_3 contains 2 tetrahedra for each octahedron, for G^t the ratio approaches the limit $a_t/b_t \rightarrow 2$ for $t \rightarrow \infty$. Mapping of a part of G^t into 3-space, tangent to a vertex of G^0 , gives onion-like clusters (Mackay icosahedra) mentioned in Section 4.3.

Another icosadeltahedron analogue is the subdivision of the facets of $\{3, 3, 5\}$ into the following four-dimensional simplicial polytope P^t having only 3 types of vertex figure (convex hull of all neighbours of a vertex): F_{20}^* , F_{24}^* and $F_{28}^*(T_d)$. The polytope P^1 is obtained from $P^0 = \{3, 3, 5\}$ by adding the center of all 600 tetrahedra and the vertices dividing each edge into 3 equal segments. This gives a decomposition of each tetrahedral facet of $\{3, 3, 5\}$ into smaller irregular tetrahedra; iteratively, P^t is obtained from P^{t-1} .

4.2.3. Triangulations, spherical wavelets

The dual t -chamfered tetrahedron, cube and dodecahedron are used for triangulations, seen as a decomposition (of the geometric domain into polyhedral elements) technique,

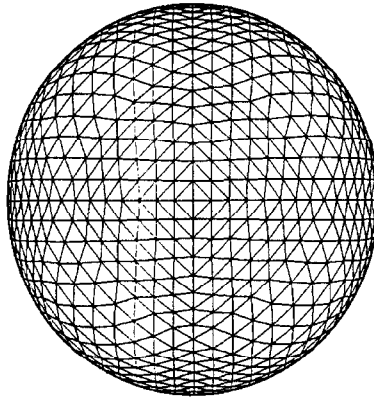


Fig. 27. Dual 4-chamfered cube \diamond_{2048}^* .

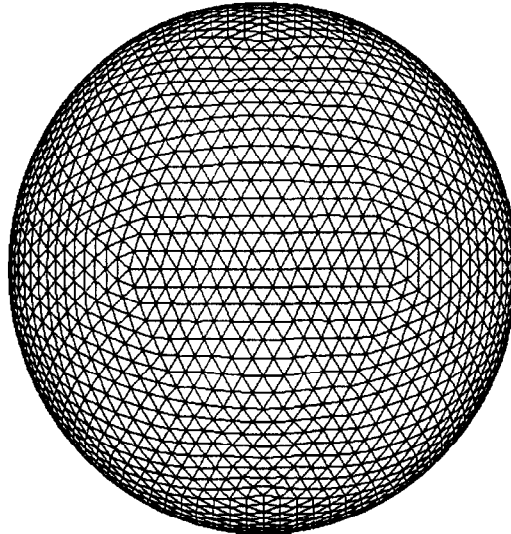


Fig. 28. Dual 4-chamfered dodecahedron $C_{5120}^*(I_h)$ (Test planetarium, Iena 1922).

in computer-aided geometric design, graphical rendering, solid modelling and finite element analysis. In particular, this is used for spherical wavelets [60,61] leading to efficient algorithms in computer graphics. For example, Schröder and Sweldens use the dual 8-chamfered dodecahedron ($20 \cdot 2^{16} = 1\,310\,720$ facets!) for a spherical texture processing of topography/bathymetry data of Earth [61]. This spherical triangulation was also considered, for example, by Gasson (see Sections 7.5 and 7.6 of [32]) (Figs. 27 and 28)

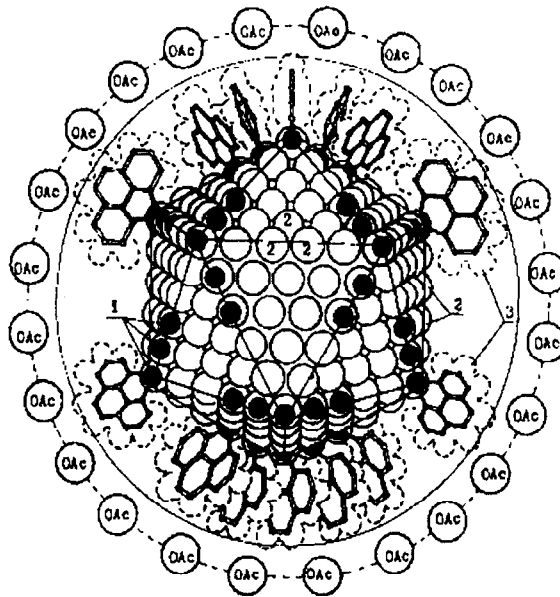


Fig. 29. Palladium icosahedral 5-cluster $Pd_{561}L_{60}(OAc)_{180}$.

4.3. Onion-like metallic clusters

4.3.1. Icosahedral and cuboctahedral metallic clusters

Besides virus capsids and geodesic domes, the dual $(a, 0)$ -dodecahedra also occur as levels (concentric *onion skins*) in some large metallic clusters [38, p. 241]). Those γ -clusters are made up of γ successive shells of atoms surrounding a central atom, each shell being either a dual $(a, 0)$ -dodecahedron or a dual $(a, 0)$ -rhombic dodecahedron. Since an icosahedral shell $C_{20a^2}^*(I_h)$ or a cuboctahedral shell $RhomDode_{20a^2}^*(O_h)$ have $10a^2 + 2$ atoms, the γ -cluster contains

$$1 + \sum_{a=1}^{\gamma} (10a^2 + 2) = \frac{(2\gamma + 1)}{3} (5\gamma^2 + 5\gamma + 3)$$

atoms. For example, the 561 palladium atoms of $Pd_{561}L_{60}(OAc)_{180}$ where conjectured in 1985 to realize the icosahedral 5-cluster; it was proved in 1996 by Vagraftik [69] (see Fig. 29, taken, with kind permission, from [38]). While the 1, 2, 4 and 5-clusters are realized (see Table 7) a metallic 3-cluster realization is, not known yet.

The evidence for γ -clusters was also observed as maxima for concentration profiles of cluster spectra in an inert gas, and was called *Mackay icosahedra*. See [22] for xenon 3, 4 and 5-clusters and see [31] for argon 3, 4, 5 and 6-clusters.

4.3.2. Other metallic clusters

Metallic clusters can also be realized by tetrahedral, octahedral or cubic shells (see, e.g. [66]). The first 5 metallic clusters given in Table 8 are made of only one shell. The

Table 7
Icosahedral and cuboctahedral metallic clusters

γ	Outer shell	Total # of atoms	Metallic cluster
1	$C_{20}^*(I_h)$	13	$[Au_{13}(PMe_2Ph)_{10}Cl_2]^{3+}$
2	$RhomDode_{60}^*(O_h)$	55	$Au_{55}(PPh_3)_{12}Cl_6$
4	$RhomDode_{320}^*(O_h)$	309	$Pt_{309}(Phen)_{36}O_{30\pm 10}$
5	$C_{500}^*(I_h)$	561	$Pd_{561}L_{60}(OAc)_{180}$

Table 8
Some metallic clusters

γ	Outer shell	Total # of atoms	Metallic cluster
1	Δ_4^*	4	$[H_2Os_4(CO)_{12}]^{2-}$
2	Δ_{16}^*	10	$[Os_{10}C(CO)_{24}]^{2-}$
3	Δ_{36}^*	20	$[Os_{20}(CO)_{40}]^{2-}$
1	\diamond_8^*	8	$[Ni_8(PPh)_6(CO)_8]$
1	\diamond_8^*	6	$Rh_6(CO)_{16}$
3	\diamond_{72}^*	44	$[Ni_{38}Pt_6(CO)_{48}H]^{5-}$

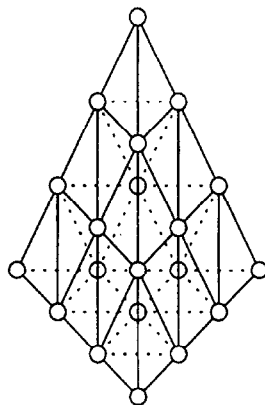


Fig. 30. Realization of the cluster $[Os_{20}(CO)_{40}]^{2-}$ as dual (3,0)-tetrahedron.

last one is made of 2 non-consecutive octahedral shells: the dual (1,0) and (3,0)-cubes \diamond_8^* and \diamond_{72}^* . Contrary to the icosahedral and cuboctahedral clusters given in Table 7, those 6 metallic clusters do not contain a central atom.

Remark 4.4 (Mackay [50]). For $\gamma \rightarrow \infty$, the infinite union with outer shell $C_{20\gamma^2}^*(I_h)$ seen as packing of the space by equal spheres is a non periodic radiating structure with a unique centre. The density of this icosahedral close packing is about

0.68818. Replacing the dodecahedron by the rhombic dodecahedron, we get the face-centred cubic lattice A_3 with (maximal among lattices) density of about 0.7405 (Fig. 30).

5. A complete list of embeddable fullerenes?

5.1. Katsura model for vesicles cells versus embeddable dual fullerenes

All known fullerenes in which the dual is ℓ_1 -embeddable — including the Voronoi plane partition of hexagonal lattice A_2 , which can be seen as C_∞ — fit the Katsura model for coated vesicles cells [43]. More precisely, the n vertices of a fullerene F_n are partitioned into 4 types $T_{a,b}$ according to the number a of pentagons and b of hexagons they are incident to, i.e., $T_{3,0}$, $T_{0,3}$, $T_{1,2}$ and $T_{2,1}$. Katsura then considers the average strain energy of its n vertices assuming Hookean elasticity and only short range interactions. The stable fullerenes, i.e., with minimal energy under his model (depending on which type of vertices have minimal energy) are the following:

The dodecahedron (minimal energy on $T_{3,0}$ vertices); its dual $F_{20}^*(I_h) \rightarrow \frac{1}{2}H_6$.

The hexagonal sheet C_∞ (minimal energy on $T_{0,3}$ vertices); its dual partition $A_2 \rightarrow \frac{1}{2}\mathbb{Z}_3$.

The buckminsterfullerene (minimal energy on $T_{1,2}$ vertices); its dual $C_{60}^*(I_h) \rightarrow \frac{1}{2}H_{10}$.

The elongated hexagonal barrel $F_{36}(D_{6h})$ (minimal energy on $T_{2,1}$ vertices); its dual $F_{36}^*(D_{6h}) \rightarrow \frac{1}{2}H_8$.

The hexakis truncated tetrahedron $F_{28}(T_d)$ (minimal energy on $T_{2,1}$ vertices); its dual $F_{28}^*(T_d) \rightarrow \frac{1}{2}H_7$.

The two other stable fullerenes (with same energy as $F_{36}(D_{6h})$ and $F_{28}(T_d)$ and also corresponding to minimal energy on $T_{2,1}$ vertices) are the *tennis ball* $F_{32}(D_3)$ and $F_{36}(D_{2d})$ whose duals are not embeddable.

Besides fitting the Katsura model, the $C_{60}(I_h)$ is a *uniquely elegant structure* — term used by the Nobel committee awarding to Curl, Kroto and Smalley the 1996 Nobel prize in chemistry for the discovery of the first fullerene: $C_{60}(I_h)$.

5.2. All embeddable fullerenes are known?

Embeddable fullerenes seem to be extremely rare; we believe that $\{F_{20}(I_h), F_{20}^*(I_h)\}$ could be the unique pair of dual ℓ_1 -fullerenes. More precisely, with M. Shtogrin, we conjecture that all embeddable fullerenes are known, i.e.

Conjecture 5.1.

(i) All ℓ_1 -embeddable fullerenes are: $F_{20}(I_h)$, $F_{26}(D_{3h})$, $F_{44}(T)$ and $C_{80}(I_h)$.

(ii) All ℓ_1 -embeddable dual fullerenes are: $F_{20}^*(I_h)$, $F_{28}^*(T_d)$, $F_{36}^*(D_{6h})$ and $C_{60}^*(I_h)$.

Acknowledgements

The authors would like to thank Gunnar Brinkmann, Victor Chepoi, Alain Dublanchet, Patrick Fowler, Branko Grünbaum, Bruce King, Thomas Liebling, Dimitrii Pasechnik, André Rassat and Tibor Tarnai for pointing out further references, computational help, advice and encouragement.

References

- [1] D. Avis, Hypermetric spaces and the hamming cone, *Canadian J. Math.* 33 (1981) 795–802.
- [2] D. Avis, M. Deza, The cut cone, ℓ_1 -embeddability, complexity and multicommodity flows, *Networks* 21 (1991) 595–617.
- [3] A.T. Balaban, X. Liu, D.J. Klein, D. Babic, T.G. Schmalz, W.A. Seitz, M. Randic, Graph invariants for fullerenes, *J. Chem. Inf. Comput. Sci.* 35 (1995) 396–404.
- [4] M. Berman, Regular faced convex polyhedra, *J. Franklin Inst.* 291-5 (1971) 329–352.
- [5] G. Brinkmann, A. Dress, A constructive enumeration of fullerenes, *J. Algor.* (1997) (to appear).
- [6] L.D. Brown, W.N. Lipscomb, Closely boron hydrides with 13 to 24 boron atoms, *Org. Chem.* 16 (1977) 2989–2995.
- [7] D.L.D. Caspar, A. Klug, Physical principles in the construction of regular viruses, *Cold Spring Harbor Symp. Quant. Biol.* 27 1–24.
- [8] H.S.M. Coxeter, Virus macromolecules and geodesic domes, in: J.C. Butcher (Ed.), *A Spectrum of Mathematics*, Auckland University Press, 1971.
- [9] V. Chepoi, M. Deza, V.P. Grishukhin, A clin d’oeil on ℓ_1 -embeddable planar graphs, *Disc. Appl. Math.* (1997).
- [10] O. Delgado, A. Dress, A. Müller, M.T. Pope, Polyoxometalates: A class of compounds with remarkable topology, *Mol. Eng.* 3 (1993) 9–28.
- [11] A. Deza, A. Dublanchet, On structure of icosahedral viruses. (in preparation).
- [12] M. Deza, V.P. Grishukhin, Hypermetric graphs, *Quarterly J. Math. Oxford* 44 (2) (1993) 399–433.
- [13] M. Deza, V.P. Grishukhin, A zoo of ℓ_1 -embeddable polytopal graphs, *Bull. Inst. Math. Acad. Sinica* (1997).
- [14] M. Deza, M. Laurent, ℓ_1 -rigid graphs, *J. Algeb. Combin.* 3 (1994) 153–175.
- [15] M. Deza, M. Laurent, *Geometry of cuts and metrics. Algorithms and Combinatorics* 15 Springer, Berlin, 1997.
- [16] M. Deza, S. Spectorov, Recognition of ℓ_1 -graphs with complexity $O(nm)$, or Football in a Hypercube, *Eur. J. Combin.* 17-2,3 (1996) 279–289.
- [17] M. Deza, M. Shtogrin, Isometric embedding of semi-regular polyhedra, partitions and their duals into cubic lattices and hypercubes, *Russian Math. Surv.* 51-6 (1996) 1193–1194.
- [18] M.B. Dillencourt, personal communication (1996).
- [19] D.Ž. Djoković, Distance preserving subgraphs of hypercubes. *J. Combinator. Theory Ser. B* 14 (1973) 263–267.
- [20] A. Dress, D. Huson, V. Moulton, Analyzing and visualizing sequence and distance data using SPLITTREE, *Disc. Appl. Math.* 71 (1996) 95–109.
- [21] V. Eberhard, *Zur morphologie der polyeder*. Leipzig (1891) (in German).
- [22] O. Eht, K. Sattler, E. Recknagel, Magic numbers for sphere packings: experimental verification in free xenon cluster, *Phys. Rev. Lett.* 47-16 (1981) 1121–1124.
- [23] J.R. Edmundson, The distribution of point charges on the surface of a sphere, *Acta Crystallog. A* 48 (1992) 60–69.
- [24] B.S. Elk, A canonical assignment of locant numbers to fular compounds - especially fullerenes - based on graph theoretical principles, *J. Chem. Inf. Comput. Sci.* 35 (1995) 152–158.
- [25] G. Fleck, Form, Function, Functioning, in: M. Senechal, G. Fleck (Eds.), *Shaping Space. A Polyhedral Approach*, Birkhäuser, Boston, 1986, pp. 151–171.
- [26] A. Florian, Extremum problems for convex discs and polyhedra, in: P.M. Gruber, J.M. Wills (Eds.), *Handbook of Convex Geometry*, Elsevier, Amsterdam, 1993, pp. 177–221.

- [27] P.W. Fowler, J.E. Cremona, J.I. Steer, Systematics of bonding in non-icosahedral carbon clusters, *Theoret. Chim. Acta* 73 (1987) 1–26.
- [28] P.W. Fowler, D.E. Manolopoulos, *An Atlas of Fullerenes*, Clarendon Press, Oxford, 1995.
- [29] P.W. Fowler, T. Pisanski, Leapfrog transformation and polyhedra of Clar type, *J. Chem. Soc. Faraday Trans. 90* (1994) 2865–2871.
- [30] F.C. Frank, J.S. Kasper, Complex allow structures regarded as sphere packings 1. Definitions and basic principle, *Acta Crystallogr.* 11 (1958) 184–190.
- [31] J. Friedman, R.J. Beuhler, Magic numbers for argon and nitrogen cluster ions, *J. Chem. Phys.* 78 (1983) 4669–4673.
- [32] P.C. Gasson, *Geometry of Spatial Forms*. Ellis Horwood, Chichester, 1983.
- [33] G. Gévay, Icosahedral morphology, in: I. Hargittai (Ed.), *Fivefold Symmetry*. World Scientific, Singapore - New Jersey - London - Hong Kong, 1992, pp. 177–203.
- [34] M. Goldberg, The isoperimetric problem for polyhedra, *Tohoku Math. J.* 40 (1935) 226–236
- [35] M. Goldberg, A class of multi-symmetric polyhedra, *Tohoku Math. J.* 43 (1937) 104–108.
- [36] D.W. Grace, Search for largest polyhedra, *Math. Comput.* 17 (1963) 197–199.
- [37] B. Grünbaum, *Convex polytopes*. Pure and Appl. Math. 16 Wiley-Interscience, New York, 1967.
- [38] S.P. Gubin, *Khimiya klusterof*. Nauka, Moscow (1987) (in Russian).
- [39] R.H. Hardin, N.J.A. Sloane, McLaren's improved snub cube and other new spherical designs in three dimensions, *Disc. Comput. Geom.* 15 (1996) 429–441.
- [40] A. Heppes Isogonal sphärischen netze, *Ann. Univ. Sci. Budapest Eötvös Sect. Math.* 7 (1964) 41–48.
- [41] F.Q. Huang, A.C. Tang, Hückel treatment of B_{32} and B_{92} , *J. Mol. Struct.* 366 (1966) 241–248.
- [42] A.V. Karzanov, Metrics and undirected cuts, *Math. Program.* 32 (1985) 183–198.
- [43] I. Katsura, Theory on the structure and stability of coated vesicles, *J. Theoret. Biol.* 103 (1983) 63–75.
- [44] J. Kepler, *Harmonice Mundi* (1619).
- [45] R.B. King, Topological aspects of chemically significant polyhedra, *J. Math. Chem.* 7 (1991) 51–68.
- [46] T.P. Kirkman, *Liverpool Proc. Lit. Philos. Soc.* 37 (1882) 65.
- [47] A.B.J. Kuijlaar, E.B. Saff, Distributing many points on a sphere, *Math. Intelligencer* 19-1 (1997) 5–11.
- [48] S. Lhuillier, *De relatione mutua capacitatis et terminorum figurarum, etc. Varsaviae* (1782).
- [49] A. Loeb, *Space Structures: Their Harmony and Counterpoint*, Addison-Wesley, Reading, MA, 1976.
- [50] A.L. Mackay, A dense non-crystallographic packing of equal spheres, *Acta Crystallog.* 15 (1962) 916–918.
- [51] J. Malkevitch, Properties of planar graphs with uniform vertex and face structure. Ph.D. thesis, University of Wisconsin-Madison (1969).
- [52] K. Miyazaki A mystic history of fivefold symmetry in Japan, in: I. Hargittai (Ed.), *Fivefold Symmetry*, World Scientific Singapore - New Jersey - London - Hong Kong, 1992, pp. 361–393.
- [53] R. Mosseri, J.F. Sadoc, Geodesic hyperdomes and sphere packing, *Int. J. Space Struct.* 5, 3-4 (1990) 325–329.
- [54] D. Pasechnik, personal communication (1996).
- [55] B. Plestenjak, T. Pisanski, A. Graovac, The minimal non-fullerene Voronoi polyhedra, *Match* 33 (1996) 157–168.
- [56] G. Pólya, *Induction and Analogy in Mathematics*, Princeton University Press, Princeton, 1954.
- [57] J.F. Sadoc, R. Mosseri, *Frustration géométrique*. Aléa-Saclay, Eyrolles, Paris (1997) (in French).
- [58] S.C. Sah, A generalized leapfrog for fullerene structures, *Fullerenes Sci. Tech.* 2 (4) (1994) 445–458.
- [59] D.S. Schonland, *Molecular Symmetry - An Introduction to Group Theory and its Use in Chemistry*, Gauthier-Villars, Paris, 1971.
- [60] P. Schröder, W. Sweldens, Spherical wavelets: efficiently representing functions on the sphere. *Computer Graphics Proc. SIGGRAPH 95, ACM Siggraph*, 1995, pp. 161–172.
- [61] P. Schröder, W. Sweldens, Spherical wavelets: texture processing, in: P. Hanrahan, W. Purgathofer (Eds.), *Rendering Techniques '95*. Springer, Wien, New York, 1995, pp. 252–263.
- [62] S. Shpectorov, On scale-isometric embeddings of graphs into hypercubes, *Eur. J. Combinat.* 14 (1993) 117–130.
- [63] J. Steiner, Sur le maximum et le minimum des figures, *J. Math. Berlin* 24 (1842) 93–152 and 189–250.
- [64] T. Tarnai, Geodesic domes: natural and man-made, *Int. J. Space Struct.* 11, 1–2 (1996).
- [65] T. Tarnai, Geodesic domes and fullerenes. *Phil. Trans. Roy. Soc. London A* 343 (1993) 145–154.
- [66] B.K. Theo, N.J.A. Sloane, Magic numbers in polygonal and polyhedral clusters, *Inorg. Chem.* 24 (1985) 4545–4558.

- [67] B.H.S. Thimmappa, Low valent metal clusters - an overview, *Coord. Chem. Rev.* 143 (1995) 1–34.
- [68] L. Ulický, T.J. Kemp, *Comprehensive Dictionary of Physical Chemistry*, PTR Prentice-Hall, Englewood Cliffs, NJ, 1992.
- [69] M.N. Vagraftik, Gigantic clusters of palladium, *Coord. Chem.* 22–5 (1996) 352–357 (in Russian).
- [70] A.W. Wells, *Structural Inorganic Chemistry*. IV ed. Oxford, 1984.
- [71] V.A. Zalgaller, *Convex polyhedra with regular faces*. Seminar in Mathematics of V. A. Steklov Math. Institute, Leningrad 2 Consultants Bureau, New York, 1969.